EFFECTS OF PARTIAL COMPLETION ON PRODUCTIVITY INDEX

A

THESIS

Presented To The Graduate Faculty Of African University Of Science And Technology

In Partial Fulfilment Of The requirements For The Degree Of:

MASTER OF SCIENCE IN PETROLEUM ENGINEERING

By:

Ohenewaa Kakra Dankwa

AUST (Abuja-Nigeria)

December, 2011

EFFECTS OF PARTIAL COMPLETION ON PRODUCTIVITY INDEX

A THESIS APPROVED BY THE PETROLEUM ENGINEERING DEPARTMENT

RECOMMENDED: ……………………………………………………….

Chair, Dr. Alpheus Igbokoyi

……………………………………………………….

Professor Djebbar Tiab

……………………………………………………….

Professor David ogbe

APPROVED: ……………………………………………………….

Chief Academic Officer

……………………………………………………….

Date

TABLE OF CONTENTS

LIST OF FIGURES

LIST OF TABLES

ABSTRACT

A new method for analysing productivity index (PI) on vertical wells is the main objective of this study. Well performance is often measured in terms of the well's productivity which is dependent on a number of factors such as the reservoir's configuration, the type of completion, petrophysical and fluid properties, formation damage, etc. The effect of partial completion is the main focus of making the productivity index analysis since almost all vertical wells are partially completed due to the reasons of water coning or gas cap issue, etc. It is also very expensive to fully complete a well especially when the formation thickness is so large.

Pressure behaviour solutions for both closed boundary and constant pressure boundary have been obtained, taking into consideration the effect of partial completion.

Productivity of a well is usually evaluated on the long time performance behaviour, thus the pseudo-steady state (late time) approach has been employed for calculation of the productivity index.

Several key factors have been tested on productivity index such as pseudo skin, shape factors, penetration ratio, reservoir drainage area and etc. The effects of these factors have been analysed on PI. Theoretical data were used in carrying out the analysis with results indicating that, productivity index increases with increasing completion interval and vice versa, whiles pressure drop due to skin as a result of restricted entry to fluid flow increases tremendously with decreasing completion interval.

Shape factors of various well positions in bounded reservoirs were computed and compared with results obtained by Dietz, and Babu and Odeh.

CHAPTER ONE

INTRODUCTION

1.1   PROBLEM STATEMENT

Well productivity is one of the major concerns in oil field development, and provides the means for oil field development strategy. Sometimes, well performance is measured in terms of productivity index. In order to arrive at the economic feasibility of drilling a well, petroleum engineers require proven and reliable methods to estimate the expected productivity of that well. Well productivity is often evaluated using the productivity index, defined as the production rate per unit pressure drawdown. Petroleum engineers often relate the well productivity evaluation to the long-time performance behaviour of a well, that is, the behaviour during pseudo-steady-state or/and steady-state flow of a closed system or/and constant pressure system respectively.

The long-term productivity of oil wells is influenced by many factors. Among these factors are petrophysical properties, fluid properties, degree of formation damage and/or stimulation, well geometry, well completions, number of fluid phases, and flow-velocity type (Darcy, non-Darcy) (Yildiz, 2003).

Depending upon the type of wellbore completion configuration, it is possible to have radial, spherical or hemispherical flow near the wellbore. A well with a limited perforated interval (partial completion) could result in spherical flow in the vicinity of the perforations as depicted in fig. 2.1. A well which only partially penetrates the pay zone, could result in hemispherical flow. These conditions could arise where coning of bottom water or gas cap becomes a serious issue (Ahmed, 2005). Figures 3.1 and 3.2 respectively depict the true picture of radial and spherical flow behaviour in a partially completed vertical well.

Partial completion is the completion of or flow from less than the entire producing interval. This situation causes a near-well flow constriction that result in a positive skin effect in a well-test analysis. The net result of partial completion yields extra pressure drop in the near wellbore region and reduces the well productivity.

The present analytical method of evaluating productivity index in vertical wells with partial completion does not account for the effect of pressure drop due to partial completion.

The purpose of this study is to develop analytical model for evaluating productivity index (P.I) of vertical wells with partial completion, where the effect of pressure drop due to partial completion is taken into account and compare results with conventional methods.

The partial differential equations were solved for both no-flow boundary and constant pressure boundary systems in Laplace and Fourier Transform domains before inversion to real time domain.

1.3   OBJECTIVES

The main objectives of this work are to:

- Develop analytical model for pressure behaviour in closed and constant pressure boundary systems
- Develop an analytical model for evaluating productivity index of vertical wells with partial completion for both closed-boundary and constant pressure boundary systems taking into account the effect of pressure drop due to partial completion
- Calculate shape factors and compare with the existing ones and
- Investigate the factors and parameters that influence or control productivity index.

1.4   METHODOLOGY

The partial form of the diffusivity equation in dimensionless terms is solved for both closed system and constant pressure boundary case employing Laplace and Fourier transforms. Gringarten and Ramey's source functions (1974) for closed and bottom water drive (mixed boundaries system) have been used in conjunction with Babu and Odeh's approach (1989) for obtaining pressure drawdown in terms of average reservoir pressure. Finally new productivity index equations are generated for both closed system and bottom water drive of a vertical well with partial completion.

1.5   WORK OUTLINE

This work is made up of seven chapters; chapter one consists of the problem statement, objectives and methodology used to solve the problem. Chapter two covers the literature review. Chapter three is dedicated to the pressure behaviour for closed-boundary and constant pressure boundary systems, whiles chapter four presents the theoretical model of productivity index and shape factor for partially completed vertical wells and their applications. Chapter five presents the factors which

influence productivity index and their effects. Chapter six covers discussion of results and finally, chapter seven gives conclusions and recommendations for future research in this area.

CHAPTER TWO

LITERATURE REVIEW

2.1   PARTIAL COMPLETION/PENETRATION

The problem of partial penetration was first studied by Muskat for steady-state conditions where he calculated pressure distributions and productive capacities for anisotropic formation (Muskat, 1932). His conclusion was that, the productivity depended slightly on the directional permeability

ratio $\frac{kz}{kr}$ >0.1.   (2.1)

Studies were carried out on electrical analogue experiments on the effect of casing perforation completions on well productivity for ideal uniform reservoirs under steady-state homogeneous conditions. Results were presented graphically for the effect of perforations of different densities and various degrees of penetration into the formation surrounding the casing or cement sheath. It was found that the penetration of the perforations into the surrounding productive section may so increase the resultant productivity as to approach or even exceed that for open-hole completions. That is, if the perforations are long enough, the productivity of a perforated well might be even higher than that of an open-hole (McDowell and Muskat, 1950).

Nisle (1958) employed the instantaneous point source solution to the diffusivity equation to solve the constant flux, isotropic and partial penetration problem. From his synthetic pressure build up curves for various penetration ratios constructed, he found that the theoretical build up curves consisted of two semi-log straight line portion: an early straight line having a slope inversely proportional to the flow capacity of the open interval k_{hw}, a later semi-log straight line which had a slope inversely proportional to the flow capacity of the entire thickness of the formation k_h.

Odeh (1968) employed a finite cosine transform to arrive at a solution for his steady-state flow problem; the open interval was located anywhere within the producing interval.

Kazemi and Seth (1969) also concerning the issue of partial-penetration problem for an infinite conductivity inner boundary condition used numerical finite difference model to arrive at their solution.

The exact solution of the partial penetration problem presents great analytical problems because the boundary conditions that the solutions of the PDE's must satisfy are mixed, that is, on one of the boundaries; the pressure is specified on one portion and the flux on the other. This difficulty occurs at the well bore, for the flux over the non-productive section of the well is zero, and the potential over the perforated interval must be constant. In the case of constant rate production from the well, this uniform potential (pressure) is time dependent and unknown, and the additional condition that;

$$\int \left(\frac{dp}{dr}\right) dz = \text{a constant,} \tag{2.2}$$

(Limit from h_1 to zero) where h_1 is the thickness of perforated interval, must also be satisfied (Clegg and Mills, 1969).

Gringarten and Ramey (1974) also worked on the infinite conductivity partial-penetration problem employing the finite Difference model. The numerical scheme chosen consisted of second-order-correct central difference approximation of the space derivative and the Crank-Nicolson implicit procedure using a second-order-correct implicit procedure forward difference approximation of the time derivative.

The basic radial flow equations are derived with assumption that the well is completed across the entire producing interval signifying fully radial flow. The flow cannot be any longer termed radial if the well partially penetrates the formation. The flow description of the restricted region is more spherical, thus it becomes clear that the behaviour of flow is influenced by permeability both in radial and vertical direction (Kr and Kz respectively).

2.2   PRODUCTIVITY LOSS (I)

Brons and Martings (1961) came up with two important parameters which are paramount in the study of loss in productivity (*I*) in all the three cases under fig. 2.1 thus, penetration ratio, b and ratio $\dfrac{h_s}{r_w}$.

Where:

h_s is the height of a symmetry element within the total zone thickness,

r_w is the well bore radius

The productivity loss is given by;

$$I = \frac{S}{\ln\left(\dfrac{r_e}{r_w}\right) - 0.75 + S}$$

(2.3)

The fractional loss in productivity, I is related to the skin factor S_b Based on this relation, I is a function of Sb, for r_e=660 ft, and r_w=3 in. according to a graph put up by Brons and Martings (1961).

In their conclusion, considering the figure 2.1 (A, B, C) it can be seen that all cases have their penetration ratios to be 0.2, however, $\dfrac{h_s}{r_w}$ is 600, 300, and 60 respectively. It follows from their graph that for re=660 ft and r_{ew}=3 in., the loss in productivity is 68, 65 and 11 per cent respectively. From these results, it is clear to conclude that better productivity is obtained from an interval open in the middle of a production zone than from the same open interval located at either the top or bottom of the zone.

Additionally, they added that, the larger the number of intervals for a given total penetration ratio, the higher the productivity will be.
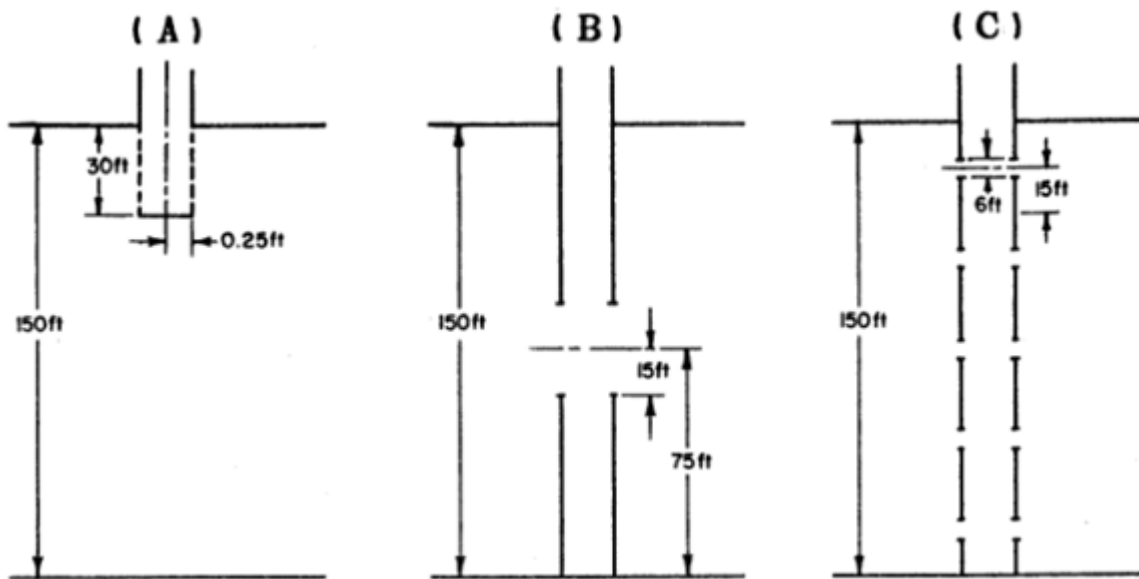
Figure 2.1 Partial Completions and Partial Penetration from Brons and Martings (1961)

h= formation thickness

h_p= perforated thickness

Penetration ratio, b= $\dfrac{h_p}{h}$

h_s=thickness of a symmetry element

Dimensionless thickness= $\dfrac{h_s}{r_w}$ (2.4)

$$h_D = \sqrt{\dfrac{k_r}{k_z}} * \dfrac{h_s}{r_w}$$ (2.5)

It is realized that, the distortion of the flow streamlines from the fully radial case will be great in case A which has the highest h_s, and least in case C.

Pseudo skin S_b accounting for partial completion can be determined from the values of b, and $\dfrac{h_s}{r_w}$ using a graphical approach employed by Brons and Martings whose analyses were based on isotropic permeability distribution where $k_r = k_z$. This is always not the case, as most times $k_z < k_r$ thus, this method underestimates the pseudo skin due to partial completion in anisotropic formation.

This problem of underestimation may be overcome in the case of constant rate production by making the assumption that the flux into the well is uniform over the entire perforated interval, so that on the well bore the flux is specified over the total formation thickness (Mills and Clegg, 1969). The authors noticed that, the approximation naturally lead to an error in the solution since potential (pressure) will not be uniform over the perforated interval. From their results obtained, however, it will be seen that, this occurrence is not too significant. This uniformly distributed flux into the well is equivalent to the assumption used by Brons and Martings, and Muskat that, the well is a "line-source".

2.3   PSEUDO-SKIN FROM PARTIAL COMPLETIONS

Brons and Martings (1961) came up with pseudo-skin either caused by a partially penetrated or limited- entry line source well whose results compared closely with that of Muskat's.

Brons and Martings (1961) have also shown that the deviation from radial flow due to restricted fluid flow entry leads to an additional pressure drop close to the well-bore which can be interpreted as an extra skin factor. This is because the deviation from radial flow occurs in a very limited region around the well and changes in rate, for instance, will lead to an instantaneous perturbation in the additional pressure drop without any associated transient effect (Heriot-Watts University, 1998). The pseudo skin can be determined as a function of two parameters; the penetration ratio, b, and the ratio $\dfrac{h_s}{r_w}$.

7

$$b = \frac{h_p}{h} = \frac{total\ interval\ open\ to\ fluid\ entry}{total\ thickness\ of\ producing\ zone} \qquad (2.6)$$

Three possible completion types' scenarios are portrayed here by Brons and Martings (1961) as depicted in Fig. 2.1. It considers a well in which part of the productive formation is blocked off completely either by incomplete penetration or by exclusion of parts of the productive zone by blank casing.

Fig. 2.1(A) describes a well which only partially penetrates the formation. This is often done to combat the actual or imagined danger of bottom water coning.

Fig. 2.1(B) shows a well producing from only the central portion of the productive interval. This type of completion is sometimes used where both water and gas coning are a problem. This case would be described later in this work.

Fig. 2.1(C) shows several intervals open to production.

In fig. 2.1(A), flow lines in the upper most portion of the formation will be essentially horizontal, while those in the lower portion will curve toward the well

When the centre portion of the production zone is open to production, as depicted in the fig. 2.1(B), the streamlines configuration of the upper half will be an exact mirror image of that in the lower half of the zone; therefore h, is defined as one-half the total of sand thickness.

Fig. 2.1(C) follows that, h is one-half the distance between corresponding points in adjacent intervals.

"Pseudo" skin factor;

$$S_b = \frac{1-b}{b}\ (\ \ln\left(\frac{h}{rw}\right)\text{-G(b))} \qquad (2.2)$$

Where, G(b) is a function of b obtained numerically.

Saidikowski (1979) presented a method to aid in the interpretation of well tests which yields estimates for the components which contribute to the skin factor. The skin factor is composed of two components, one which is indicative of actual formation damage and the other, which results from an additional pressure drop due to partial completions. The skin factor measured in build-up tests does not reflect the simple sum of these two components; rather, the effect of the actual damage is accentuated by the partial-completion. It was realised that partial-penetration greatly magnifies the effect of formation damage. The skin effect determined from a well test in such a case must be carefully examined, particularly if the value of the skin factor will enter into the

8

decision for stimulation or work-over treatments. To measure true damage, S_d, the completion interval, h_p, and total formation interval, h_t, must be known.

Frequently when wells are completed; the height that is open to the formation is smaller than the reservoir height (Economides, 1993). This is also known as partial penetration. Wells may be completed partially in order to: delay or avoid water/gas coning, reduce cost of completing entire productive interval, and meet surface storage capacity. Poor perforation work on the entire zone may often seem as partially completed.

In modern reservoir testing practices, partial penetration may be created to form early-time spherical flow to allow calculation of vertical permeability. Late-time radial flow would have the distinguishing characteristics of partial completion [Economides, 1993]

The nature of flow lines (bending) result in a skin effect, thus, the smaller the perforations (interval), compared to the reservoir height, the larger the skin effects would be.

Economides made an analogy that if completed interval is 75% of the reservoir height or more, this skin effect becomes negligible. While partial completion generates a positive skin by reducing the well exposure to reservoir, a deviated well results opposite.

Yildiz (2003) presented methods to predict the total skin factor for perforated and damaged wells, and the non-linear interaction between individual skin components. He showed that the total skin factor models based on the simple addition of individual skin factors due to formation damage, perforation, inclination, partial penetration etc. do not work.

2.4   PRESSURE TRANSIENT TESTING

Tiab et al (2005) presented an approach of assessing reservoir performance by measuring flow rates and pressures under a range of flowing conditions and applying the data to a mathematical model. Input data during test include; reservoir height and fluid properties. The resulting outputs typically include an assessment of reservoir permeability, the flow capacity of the reservoir, and any damage that may be restricting productivity. Pressure-transient testing is usually synonymous to well testing. The most common practice to analyse pressure transient data is to assume a radial flow profile. However, in wells with partial penetration/completion, a hemispherical/spherical flow is more representative of the system. In reality, the formation itself is usually non-uniform or heterogeneous in properties such as porosity and permeability, both areally and vertically resulting from deposition, folding or faulting. The

vertical anisotropy is fundamental in describing pressure response around a well partially penetrating a formation unbounded laterally and confined at the top and bottom by impermeable layers.

Tiab et al (2005) again presented a study to identify on the pressure and pressure derivative curves the unique characteristics for different flow regimes resulting from these types of completions and to determine various reservoir parameters, such as vertical permeability, horizontal permeability, and various skin factors. The interpretation is performed using Tiab Direct Synthesis (TDS) Technique, introduced by Tiab (1993), which uses analytical equations obtained from characteristic lines and points found on the log-log plot of pressure and pressure derivative to determine permeability, skin and wellbore storage without using type-curve matching. It was found that a spherical or hemispherical flow regime occurs prior to the radial flow regime whenever the penetration ratio of about 20%. A half-slope line on the pressure derivative is the unique characteristic identifying the presence of the spherical/hemispherical flow. The typical half-slope line of theses flow regimes is used to estimate spherical permeability and spherical skin values. These parameters are then used to estimate vertical permeability, anisotropy index and skin.

2.5   FLOW GEOMETRIES

Pressure-transient testing is a descriptive well testing. Estimation of the formation's flow capacity, characterization of well-bore damage and evaluation of a
Work-over or stimulation treatments all require a transient test because a stabilised test is unable to provide unique values for mobility-thickness and skin. Transient tests are performed by introducing abrupt changes in surface production rates and recording the associated changes in bottom-hole pressure. Production changes, carried out during a transient well test, induce pressure disturbances in the well-bore and surrounding rock. These pressure disturbances travel into the formation and are affected in various ways by rock features. For example, a pressure disturbance will have difficulty entering a tight reservoir zone, but will pass unhindered through an area of high permeability. It may diminish or even vanish upon entering a gas cap. Therefore, a record of well-bore pressure response over time produces a curve whose shape is defined by the reservoir's unique characteristics. Unlocking the information contained in pressure transient curves is the fundamental objective of well test interpretation (Schlumberger, 1998).

Typical pressure responses might be observed with different formation characteristics such as homogeneous reservoir, double porosity reservoir or impermeable boundary. A plot consists of

two curves presented as log-log graphs. The top curve usually represents the pressure changes associated with an abrupt production rate perturbation, and a bottom curve (termed the derivative curve) indicates the rate of pressure change with respect to time. Its sensitivity to transient features resulting from well and reservoir geometries (which are virtually too subtle to recognize in the pressure change response) makes the derivative curve the single most effective interpretation tool. However, it is always viewed together with the pressure change curve to quantify skin effects that are not recognised in the derivative response alone.

Pressure transient curve analysis probably provides more information about reservoir characteristics than any other technique. Horizontal and vertical permeability, well damage, fracture length, storativity ratio and inter-porosity flow coefficient are just a few of the characteristics that can be determined. In addition pressure transient curves can indicate the reservoir's extent and boundary details. The shape of the curve, however, is also affected by the reservoir's production history. Each change in production rate generates a new pressure transient that passes into the reservoir and merges with previous pressure effects. The observed pressures at the well-bore will be a result of the superposition of all these pressure changes.

Different types of well tests can be achieved by altering production rates. Whereas a build-up test is performed by closing a valve (shut-in) on a producing well, a draw-down test is performed by putting a well into production. Other well tests, such as multi-rate, isochronal and injection well fall-off are also possible (Schlumberger, 1998).

In a similar study, the author presents analytical models to predict the productivity of selectively perforated vertical wells. The models consider arbitrary phasing angle, non-uniform perforation size and length, and formation damage around perforations. The accuracy of the models was verified against the results from the experimental studies, the semi-analytical correlation, and the numerical models (Yildiz, 2002).

Lu (2003) presented partially penetrating wells pressure drawdown formulae in a circular cylinder drainage volume with constant pressure at edge boundary. It also provides the formulae to calculate pseudo-skin factor due to partial penetration. If the producing well length is equal to the pay zone thickness, the equations of fully penetrating wells are obtained. The primary goal of this study is to present new pressure drawdown formulae of partially penetrating wells. Analytical solutions are derived by making the assumption of uniform fluid withdrawal along the portion of the wellbore open to flow. Taking the producing portion of a partially penetrating well as a uniform

line sink, according to the point convergence pressure and the Principle of Superposition of Potential, the new well test formulae of partially penetrating wells is obtained. If both upper and lower boundaries are impermeable, when time is sufficiently long, (long after the time when pressure wave reaches the upper and lower impermeable boundaries) and let Sp denote pseudo-skin factor due to partial penetration and S_m denote mechanical skin factor due to formation damage or stimulation, the equations of dimensionless average pressure of a partially penetrating well are below:

$$P_{wD} = \left(\frac{2L_pD}{H_D}\right)\left\{Ei\left[-\left(\frac{R_{eD}^2 - R_{0D}^2}{4t_D}\right)\right] - Ei\left(-\frac{R_{wD}^2}{4t_D}\right)\right.$$
$$\left. - \left(\frac{1}{R_{oD}^2}\right)(2R_{oD}^2 - R_{eD}^2)\left[exp\left(\frac{R_{oD}^2 - R_{eD}^2}{4t_D}\right) - exp\left(-\frac{R_{eD}^2}{4t_D}\right)\right]\right\} + S_p$$
$$+ S_m \qquad\qquad (2.7)$$

Tiab et al (2005) have shown that vertical wells can exhibit different flow regimes during their transient behaviour. Spherical flow can occur when a well is producing from a limited section of a thick reservoir or producing from a thick reservoir under a variety of conditions such as the presence of shale barriers. In the case of partial completion in thick reservoirs, spherical flow can be visualized as flow along the radius of a sphere; the concept of perfect radial flow towards a common point in a sphere: its centre. Hemispherical flow is identical to spherical flow with the obvious exception that the flow is contained within a hemisphere.

In practice, the flow is not purely spherical or hemi-spherical because the completion interval is not a true point sink. However, the flow is spherical in a practical sense if the completion interval is very short relative to the net pay. In the case of a thick reservoir between two impermeable confining layers and a short partial completion interval, the spherical flow regime will occur between two periods of cylindrical-radial flow. In both cases, three flow periods can be identified - additional to wellbore storage- as follows:

A period 1 corresponding to an initial radial flow over the completion interval, during this period the reservoir behaves as if the formation thickness were equal to the length of the open zone.

A Period 2 corresponds to a transition period during which spherical/hemispherical flow may be identified.

And the third period corresponds to a second radial flow but this time over the total formation thickness.

In another study, a methodology and an associated computer program were developed that allows

the computation of the pseudo skin factor for partially penetrated vertical producer wells. Five methods were selected for implementation. A sensitivity analysis and model comparison was performed. The pseudo skin factor is most sensitive to the total formation thickness, and the perforated interval length. With the same input data, the Streltsova formula results in the largest pseudo skin factor values and the Odeh formula has the smallest pseudo skin factor values. (Gui et al., 2008).

Streltsova Formula:

The pseudoskin assuming uniform flux model is given by:

$$S_p = \frac{2}{\pi b} \sum_{n=1}^{\infty} \frac{1}{2} \{\sin[n\pi(b + h_{1D})] - \sin(n\pi h_{1D})\} \cos(n\pi Z_D) K_0 \left(\frac{n\pi}{h_D}\right) \qquad (2.8)$$

$$Z_D = \frac{Z}{h_t} \qquad (2.9)$$

Odeh Formula

The Odeh correlation for pseudo-skin is given by:

$$S_p = 1.35 \left\{ \left(\frac{1-b}{b}\right)^{0.825} [ln(r_w h_D + 7) - [0.49 + 0.1 ln(r_w h_D)] ln(r_{wC}) - 1.95] \right\} \qquad (2.10)$$

r_{wC} Represents the corrected wellbore radius with respect to the position of the perforated interval and it is calculated by the following equation:

$$r_{wC} = r_w exp[0.2126(Z_{mD} + 2.753)] \qquad (2.11)$$

$$Z_{mD} = h_{1D} + \frac{b}{2} \qquad (2.12)$$

2.6   FLOW/DRAWDOWN TEST

A flow or pressure-drawdown test is conducted by producing a well at a known rate or rates while measuring changes in flowing bottom-hole pressure (BHP) as a function of time.

Drawdown tests are designed primarily to quantify the reservoir-flow characteristics, including permeability and skin factor. In addition, when the pressure- transient is affected by outer boundaries, draw-down tests can be used to establish the outer or limits of a reservoir (reservoir limit tests) and to estimate the hydrocarbon volume in the well's drainage area.

When economic considerations require a minimum loss of production time, pressure-drawdown tests also can be used to estimate the deliverability of a well and, if conducted and analyzed properly, they are viable alternatives to deliverability tests.

The basis of flow-test analysis techniques is the line-source (Ei-function) solution to the radial flow

diffusivity equation.

The relationship between flowing bottom-hole pressure, (BHP), Pwf, and the formation and well characteristics for a well producing at a constant rate is:

$$P_{wf} =$$

$$P_i + \frac{70.6qB\mu}{kh}\left[ln\left(\frac{1688\emptyset\mu C_t r_w^2}{kt}\right) - 2S\right] \tag{2.13}$$

(Lee et al, 2003)

2.7   PRESSURE BUILD-UP TESTS

Pressure-build-up tests on the other hand are conducted by first stabilizing a producing well at some fixed rate, placing a BHP measuring device in the well, and shutting in the well. Following shut-in, the BHP builds up as a function of time, and the rate of pressure build-up is used to estimate well and formation properties, such as average drainage area pressure, permeability in the drainage area of the well, and skin factor in the region immediately adjacent to the well-bore. The dimensionless shut-in pressure is given by:

$$P_{Ds} = \frac{2\pi*10^{-6}kh}{qB\mu}(P_i - P_{ws})$$

$$= P_D(t + \Delta t)_{DA}$$

$$- P_D(\Delta t_{DA}) \tag{2.14}$$

Δt_{DA}=Dimensionless shut-in time and

P_{ws}=Shut-in well pressure

The Horner method is a widely used technique to analyse pressure build-up. It involves plotting the shut-in pressure (Pws) versus the logarithm of the time ratio$\left(\frac{t+\Delta t}{\Delta t}\right)$. On dimensionless coordinates, PDs is graphed as a function of$log\left(\frac{t+\Delta t}{\Delta t}\right)$.

For fully penetration, build-up data form a straight line with slope of 1.151 per log cycle on the dimensionless Horner graph at early shut-in time.

For partially penetrating wells with closed upper and lower boundaries, two straight lines appear on the dimensionless Horner graph; the slope of the first one is proportional to the flow capacity of the open interval, khw and the slope of the second line is proportional to the flow capacity of the entire formation, kh (Buhidma and Raghavan, 1980).

2.8 Basic Concepts of Pressure Transient Analysis

There are a number of concepts that are basic to the formulation and practical application of the classical well test model. These include the following:

· Infinite-acting reservoir

· A Finite reservoir with closed boundaries

· A Finite reservoir with constant pressure boundaries

· Effective drainage radius

· Radius of investigation

· Time to stabilization

· Wellbore storage

2.8.1 Infinite-Acting Reservoirs

The concept of an infinite-acting or infinitely large reservoir is used in implementing the outer boundary condition for the classical well test model. It describes the condition where measurable pressure transients have not travelled far enough to reach the closest reservoir boundary. In radial-cylindrical flow geometry, the infinite-acting reservoir concept allows us to impose the outer boundary condition that in an infinitely large system, there is no pressure change at the external boundary:

As r_e approaches infinity, P= P_i for $t \geq 0$

This boundary condition simplifies the analytical solution. Moreover, it requires us to use the solution of the classical well test model (the exponential integral solution) only during the initial stages of testing, before the measurable pressure disturbance has reached the reservoir boundaries.

In reality, no reservoir is infinitely large. This concept does not imply, however, that the classical well test model is unrealistic. No matter how small a reservoir is, there will always be an infinite-acting period during which no measurable pressure change is observed at a closest point on the boundary.

2.8.2   Finite Reservoir with Closed Boundaries

The idea of a finite reservoir with closed boundaries applies to a volumetric reservoir: a closed system in which there is no fluid flow across the outer boundaries. In other words, pressure gradients across the system's outer boundaries are zero.

Closed boundaries may result from physical permeability barriers such as sealing faults or permeability pinchouts. A no-flow boundary may also form because of a large number of well patterns drilled in a homogeneous reservoir segment. In such a case, the hypothetical no-flow boundary corresponds to the drainage area of a given well. For example, wells may be much more closely spaced along a particular direction, (y-direction) because the formation permeability in that direction is significantly less than the permeability in the other direction (x-direction).It also shows the pressure transient signifying that a measurable pressure drop has reached the outer boundary, the gradients of the pressure profiles become smaller as the reservoir is depleted.

2.8.3   A Finite Reservoir with Constant Pressure Boundaries

Constant pressure boundaries are characteristic of reservoirs connected to aquifers (i.e., bottom water drive or edge water drive), or those with associated gas caps. In these types of reservoirs, pressure remains constant at an aquifer and/or gas cap interface(s).

Hypothetical constant pressure boundaries can be formed if a production well is surrounded by injection wells, as usually depicted in a water-flooding pattern. When a pressure transient reaches the outer boundary of a constant pressure boundary reservoir, the flow across the boundary must be equal to the flow through the well. Thus, the pressure distribution does not change over time, and the reservoir attains true steady-state conditions. Under these conditions, the well-bore experiences no further pressure decline, and the pressure at the external boundary remains at the initial pressure. Note that the tested well experiences infinite-acting flow behaviour until these steady-state conditions develop.

CHAPTER THREE

PRESSURE BEHAVIOUR IN PARTIAL COMPLETION WELLS FOR CLOSED AND CONSTANT PRESSURE BOUNDARY SYSTEMS

3.1   INTRODUCTION

This chapter presents the reservoir systems used in this work, namely: reservoir with no-flow boundary and constant pressure boundary. The basis of modern reservoir engineering lies in the quantitative description of unsteady-state, multiphase fluid flow in heterogeneous porous media under the influence of pressure, gravitational and capillary forces. In the general case the flow pattern is spatially three-dimensional and three separate phases namely oil, water and gas may be flowing simultaneously in the reservoir.

The solution of such formidable flow problems can only be obtained numerically using sophisticated simulation techniques. The only redeeming feature of reservoir flow is that it is essentially laminar in nature resulting in a linear relation between local superficial fluid velocity and potential gradient.

However, in certain circumstances the reservoir flow is much simpler in character and can be modelled on a reduced basis involving only one space dimension, one mobile phase and one prevailing force (Heriot Watts University, 1998).

The radial flow is the flow pattern which best describes what actually takes place in around a well open to flow in an oil zone. Before any water break-through and if the pressure everywhere in the reservoir is above the bubble point, the only flowing phase is the oil phase. The issue of connate water is withheld by the capillary force. The radial flow is best described as horizontal flow and one-dimensional assumption is a good approximation in a situation where there is no water/gas coning. This flow system has an influence also the well's productivity index, which a measures of the ratio of the oil rate to some pressure drawdown.

3.2   GENERAL OVERVIEW OF RESERVOIR FLOW SYSTEMS

Obviously, reservoirs are not really in extent, thus the infinite acting radial flow period cannot last indefinitely. Eventually the effects of the reservoir boundaries will be felt at the well being tested. The time at which the boundary effect is noticed is dependent on several factors, including the distance to the boundary, the properties of the permeable formation, and the fluid that fills it. The two types of reservoir boundaries that are commonly considered are:

- Impermeable (No flow) and

- Constant Pressure

An impermeable boundary, also known as a closed boundary, occurs where the reservoir is sealed and no flow occurs. No flow boundaries also arise due to the interference between wells (Horne, 1990).

3.2.1   Classification of Reservoir Flow Systems

Reservoir flow systems are usually grouped according to:

- The type of fluid

- The geometry of the reservoir or portion thereof and

- The relative rate at which the flow approaches a steady state condition following a disturbance

For most engineering purposes, the reservoir may be classified either as:

1. Incompressible

2. Slightly compressible or

3. Compressible

The flow systems in reservoir rocks are classified according to their time dependence, as steady state, transient, late transient, or pseudo steady state.

During the life of a well or reservoir, the type of system can change several times, which suggests that it is critical to know as much about the flow system as possible in order to use the appropriate model to describe the relationship between the pressure and the flow rate (Craft and Hawkins, 1991).

3.2.2   Reservoir Flow Geometry System (Radial Flow)

The flow geometry of a homogeneous reservoir system is presented by radial flow. The flow of reservoir fluids into and away from the wellbore will take a radial pattern due to the absence of any serious heterogeneity. In a radial flow, fluid move towards the well from all directions and congregate at the wellbore as shown in figure 3.1.
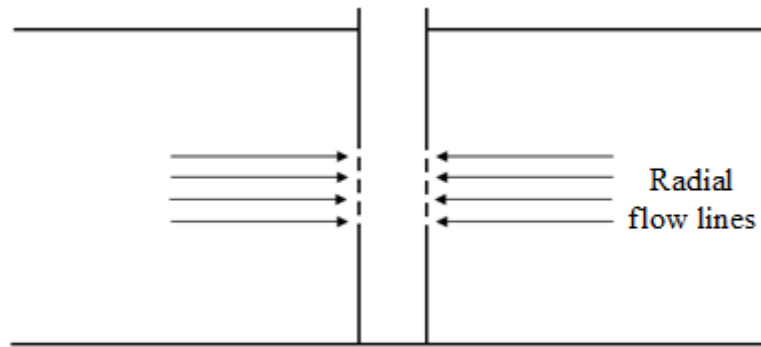
Figure 3.1 Radial Flow as a result of Partial Completion

3.2.3   The Spherical Flow Regime of well with partial completion

For well with partial completion, the well is in contact with the producing interval on a fraction only of the pay thickness, thus the well's surface contact being reduced.

For such a well, after an initial radial flow regime in front of the perforated interval, the flow lines are established in both the horizontal and vertical directions until the top and bottom boundaries are reached. A spherical flow regime can therefore be observed before the flow becomes radial in the complete formation thickness. The spherical flow is described in figure 3.2.
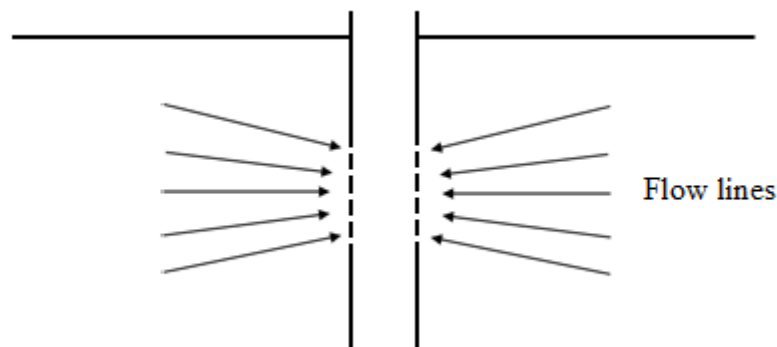
Figure 3.2 Spherical Flow as a result of Partial Completion

3.3   CLOSED SYSTEM

A closed system behaviour is a characteristic of limited reservoirs but it can also be encountered in developed fields, when several wells are producing and each well drains only a certain volume of the reservoir (Matthews and Russell, 1967).

When a reservoir (or a well's own "drainage region") is closed on all sides, the pressure transient will be transmitted outward until it reaches all sides, after which the reservoir depletion will enter the state known as the pseudo steady state. In this state, the pressure in the reservoir will decline

at the same rate everywhere in the reservoir (or drainage region).

For the closed system model, the reservoir is described as closed in all areas. It is important to note that the responses are different for a drawdown and a build-up. During drawdown periods, when all boundaries have been reached after the infinite acting behaviour, the reservoir starts to deplete. The response follows the pseudo steady state flow regime, and the well flowing pressure becomes proportional to time. During build-ups, the shape of the well response is different. After shut-in, the pressure starts to build-up during the initial infinite regime but, later, it stabilizes and tends towards the average reservoir pressure $\bar{P}_R$.

Thus a pseudo steady state is not at all steady, and corresponds to the kind of pressure response that would be seen in a closed tank from which fluid was slowly being removed (Horne, 1990).

3.3.1 Pseudo steady state Flow

The pseudo steady state flow is also known commonly as the semi steady state flow in a reservoir. When the pressure at different locations in the reservoir is declining linearly as a function of time, i.e., at a constant declining rate, the flowing condition is characterized as the pseudo steady-state flow. Mathematically, this definition states that the rate of change of pressure with respect to time at every position is constant, or $\frac{\partial P}{\partial t} = c$ (Ahmed, 2005). Thus, the difference between the average reservoir pressure and the pressure in the wellbore approaches a constant with respect to time.

3.3.2 General Characteristic flow regimes

When the lower and upper boundaries are impermeable, three characteristic regimes can be observed after the wellbore storage early time effect as depicted in figure 3.3.

1. Radial flow occurs over the perforated interval h_p with ΔP proportional to log (Δt) and a first derivative plateau. Analysis of the initial radial flow regime yields the permeability-thickness product for the open interval $k_h h_p$ and the infinitesimal skin of the well, S_m.

2. Spherical flow with ΔP proportional to $\Delta t^{-0.5}$ and a negative half slope straight line on the derivative log-log curve. The spherical flow regime lasts until the lower and upper boundaries are reached. Analysis yields the permeability anisotropy, $\left(\frac{k_z}{k_r}\right)$.

3. Radial flow over the entire reservoir thickness with ΔP proportional to $log\Delta t$ and a second derivative stabilization. The reservoir permeability-thickness product $k_h h$ and the total skin

can be estimated from the second radial flow regime. (Dominique, 2002).

3.3.3 Closed System Reservoir and Well Models

Considering a vertical well partially completed in the middle with no flow boundary at the top and bottom as shown in figure 3.3 below.
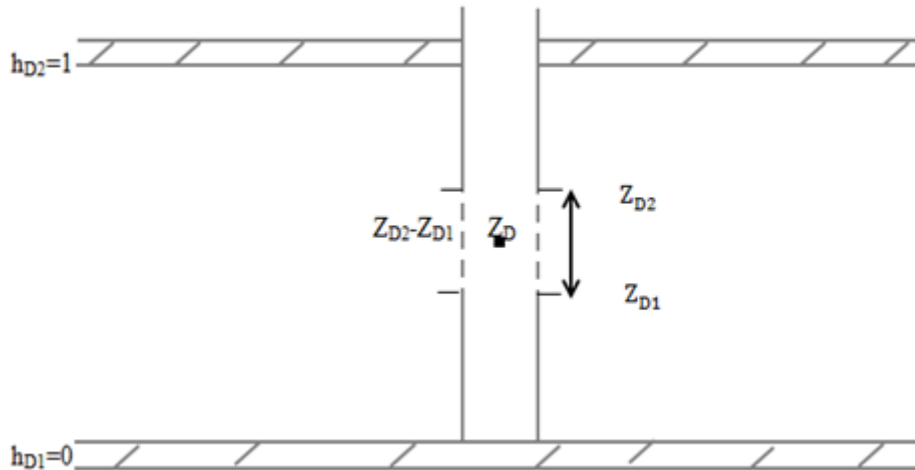
Fig. 3.3 Schematic showing a partially completed well at its centre

The completion interval is between z_{D1} and z_{D2}, z_D is the dimensionless length in the vertical direction.

For partial completion model, the diffusivity equation can be written as:

$$\frac{\partial^2 P_D}{\partial r^2{}_D} + \frac{1}{r_D} \cdot \frac{\partial P_D}{\partial r_D} + \alpha \frac{\partial^2 P_D}{\partial z^2{}_D} = \frac{\partial P_D}{\partial t_D} \tag{3.1}$$

The following assumptions are made in the derivation of the equation

- At time t=0, the pressure is uniformly distributed in the reservoir, equal to the initial pressure P_i. The reservoir is with finite uniform thickness, h, while the productive interval is h_p which spans across the completed interval.

- The well is taken as a uniform line source, the drilled well length is h, the producing well length is h_p which spans across the completed interval and the wellbore radius is r_w.

- There is a single phase fluid, of small and constant compressibility, constant viscosity μ, and formation volume factor, which flows from the reservoir to the well. Fluid properties are not dependent on pressure and gravity and capillary forces are negligible.

- There is no water encroachment or water/gas coning and multiphase flow effects are ignored.

If the reservoir is with top and bottom impermeable boundaries, i.e., the boundaries at h_{D1}=0 and

$h_{D1}=1$ are both impermeable, e.g. the reservoir does not have gas cap drive or bottom water drive, then:

$$\left(\frac{\partial P_D}{\partial z_D}\right)_{Z_D=0 \; and \; 1} = 0 \tag{3.2}$$

Inner boundary condition

$$C_D \frac{\partial P_{wD}}{d_{tD}} - \left(r_D \frac{\partial P_D}{\partial r_D}\right)_{r_{D=1} \quad z_{D1}\le z_D\le z_{D2}} = 1 \tag{3.3}$$

$$P_{wD} = P_D - S\left(r_D \frac{\partial P_D}{\partial r_D}\right)_{r_{D=1}} \tag{3.4}$$

Outer Boundary Condition

$$\left(\frac{\partial P_D}{\partial r_D}\right)_{r=reD} = 0 \tag{3.5}$$

With the application of these boundary conditions for a closed system and the use of Laplace and Fourier Transforms, a dimensionless pressure equation is obtained as:

$$\bar{P}_{wD} = \frac{x}{C_D u^2 y} + \frac{1}{h_{fD}}\sum_{n=1}^{\infty}\frac{1}{n\pi u}\left(\frac{[\sin n\pi z_{D2} - \sin n\pi z_{D1}]a}{C_D ub}\right)cos(n\pi z_D) \tag{3.6}$$

Where;

$$x = \left[K_1(r_{eD}\sqrt{u})I_0\sqrt{u} + K_0\sqrt{f}I_1(r_{eD}\sqrt{u}) - SK_1(\sqrt{u})(r_{eD}\sqrt{u})I_1(\sqrt{u}) + S\sqrt{f}K_1(\sqrt{u})I_1(r_{eD}\sqrt{u})\right]$$

$$y = \left[K_1(r_{eD}\sqrt{u})I_0\sqrt{u} + K_0\sqrt{f}I_1(r_{eD}\sqrt{u}) - SK_1(\sqrt{u})(r_{eD}\sqrt{u})I_1(\sqrt{u}) + S\sqrt{f}K_1(\sqrt{u})I_1(r_{eD}\sqrt{u})\right]$$
$$- \sqrt{u}K_1(r_{eD}\sqrt{u})I_1\sqrt{u} + \sqrt{u}I_1(r_{eD}\sqrt{u})K_1\sqrt{u}$$

$$a = \left[K_1(r_{eD}\sqrt{f})I_0\sqrt{f} + K_0\sqrt{f}I_1(r_{eD}\sqrt{f}) - SK_1(\sqrt{f})(r_{eD}\sqrt{f})I_1(\sqrt{f}) + S\sqrt{f}K_1(\sqrt{f})I_1(r_{eD}\sqrt{f})\right]$$

$$b = \left[K_1(r_{eD}\sqrt{f})I_0\sqrt{f} + K_0\sqrt{f}I_1(r_{eD}\sqrt{f}) - SK_1(\sqrt{f})(r_{eD}\sqrt{f})I_1(\sqrt{f}) + S\sqrt{f}K_1(\sqrt{f})I_1(r_{eD}\sqrt{f})\right]$$
$$- \sqrt{f}K_1(r_{eD}\sqrt{f})I_1\sqrt{f} + \sqrt{f}I_1(r_{eD}\sqrt{f})K_1\sqrt{f}$$

When the issue of Skin and wellbore storage is eliminated, the dimensionless pressure becomes:

$$\bar{P}_{wD}$$

$$= \frac{-1}{u^{\frac{3}{2}}}\left[\frac{K_1(r_{eD}\sqrt{u})I_0(\sqrt{u}) + K_0(\sqrt{u})I_1(r_{eD}\sqrt{u})}{K_1(r_{eD}\sqrt{u})I_1(\sqrt{u}) - I_1(r_{eD}\sqrt{u})K_1(\sqrt{u})}\right]$$

$$+ \frac{1}{hfD}\sum_{n=1}^{\infty}\frac{-1}{n\pi u}\left[\frac{(\sin n\pi z_{D2} - \sin n\pi z_{D1})K_1(r_{eD}\sqrt{f})I_0(\sqrt{f}) + K_0(\sqrt{f})I_1(r_{eD}\sqrt{f})}{\sqrt{f}K_1(r_{eD}\sqrt{f})I_1(\sqrt{f}) - \sqrt{f}I_1(r_{eD}\sqrt{f})K_1(\sqrt{f})}\right]$$

$$\times cos(n\pi z_D) \tag{3.7}$$

Where;

u is the Laplace space variable, K_0 and K_1 are the modified Bessel K, second kind of order zero and one respectively

I_0 and I_1 are modified Bessel I first kind of order zero and one respectively.

h_{fD} is the dimensionless thickness of the ratio $\frac{h_p}{h}$, where h_p is the productive or the perforated interval of the wellbore and h being the entire formation thickness. $\sqrt{f} = \sqrt{n^2\pi^2\alpha + u}$, $h_{fD} = z_{D2} - z_{D1}$

The procedure for the derivation of the equation for the dimensionless pressure is given under appendix A1 with detailed explanation as well as the meaning of the parameters given under the nomenclature.

The application of Gaver-Stehfest algorithm (1970) was used to invert the dimensionless pressure drop in Laplace space in MATlab program. The figure 3.4 shows various plots of pressure drop and derivative versus time for a well partially completed at the middle at different skin (S) and wellbore storage values. The reservoir is a no-flow boundary system.
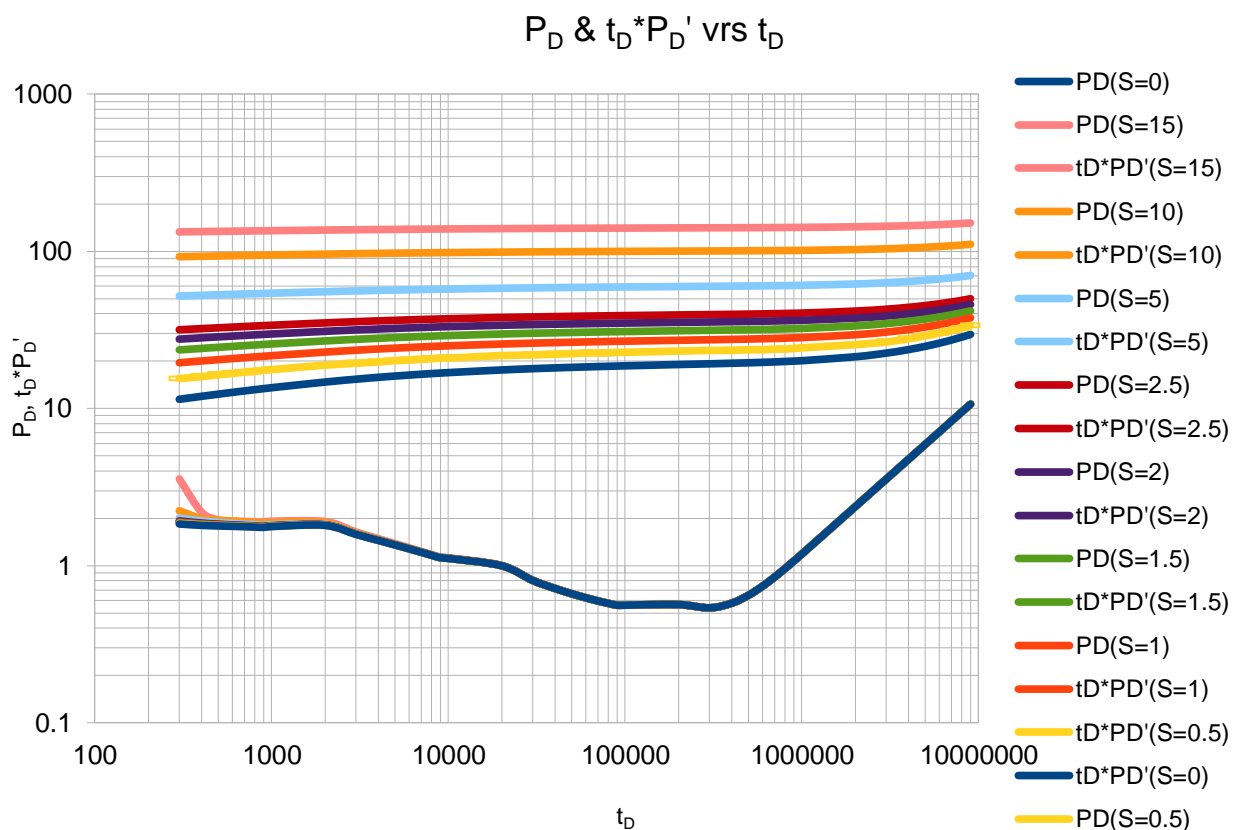
Figure 3.4 Pressure and Pressure Derivative curves for a closed boundary partial completion well

23

3.4   CONSTANT PRESSURE BOUNDARY SYSTEM

Many reservoirs are bounded on a portion or all of their sides by water-bearing rocks called aquifers. When the reservoir pressure is supported by fluid encroachment (either due to natural influx from an aquifer or a gas cap, or by fluid injection) then a constant pressure boundary may be present. Such a boundary may completely enclose the well (for example, a producing well surrounded by injectors) or may be an open boundary to one side of the well (Horne, 1990).

When the upper or lower limit of the reservoir is not sealing but at a constant pressure, such as in the case of a gas cap or a strong lower water drive, the effect of boundary is a function of the vertical permeability k_z, not the radial permeability k_r. When the well intercepts a gas cap or an aquifer, limited-entry completion or horizontal well techniques are used to prevent gas or water production. The well is opened in the oil interval away from the supporting gas or water zone and, as long as coning is not established, the high mobility of the adjacent zone maintains a fairly constant pressure at the interface with the oil-bearing interval.

A constant pressure boundary is used to describe the influence of a linear change of fluid properties, such as the presence of a gas or a water contact some distance away from an oil well. (Bourdet, 2002).

In this study, the constant pressure boundary is described for two cases namely: bottom water and peripheral water. The effect of any constant pressure boundary will ultimately cause the well pressure responds to achieve steady state at which the well pressure will be the same constant pressure as the boundary.

Thus in the description of its model characteristic after the first radial flow, if the bottom boundary or the sides (edge)is a constant pressure interface (as in the case of bottom water or peripheral water), the pressure stabilizes and the derivative drops after the spherical flow regime.

3.4.1   Steady State Flow Regime

Steady-state flow represents the condition that exists when the pressure throughout the reservoir does not change with time, $\frac{\partial P}{\partial t} = 0$. The applications of the steady-state flow to describe the flow behaviour of several types of fluid in different reservoir geometries are presented below (Ahmed, 2005). These include:

- Linear flow of incompressible fluids
- Linear flow of slightly compressible fluids

- Linear flow of compressible fluids

- Radial flow of incompressible fluids

- Radial flow of slightly compressible fluids

- Radial flow of compressible fluids

- Multiphase flow

Incompressible fluids somehow do not exist, but their properties are assumed for certain types of fluids such as heavy oil, etc., in some cases in order to derive their flow equations. Oil especially fits into the category of slightly compressible fluids due to the fact that, it exhibits small changes in its volume, or density, with changes in pressure.

3.4.2   Water and Gas Coning

The major reason for an intentional completion of well with limited entry is to minimize coning of water or gas when an oil-water or gas-oil contact is present in the well or in the area of the well. This is to prevent entry of unwanted fluid. The downward movement of pressure which occurs as a result of production from the well causes the water interface to rise towards the producing interval.

For formation of water cone, it is presumed that the bottom water is present (original oil-water contact) and the interface deforms under the influence of the pressure distribution as a result of flow (Heriot Watt University, 1998).

If an oil reservoir has both gas cap and bottom water, then the vertical well is normally perforated either near the centre of the oil zone thickness or below the centre toward the water zone. This is because coning tendencies are inversely proportional to the density difference and are directly proportional to the viscosity. Thus, density and viscosity differences between water and gas tend to balance each other. Therefore, to minimize gas as well as water coning, a preferred perforated interval is at the centre of the oil pay zone.

It is clear from the preceding discussion that coning can be reduced by minimizing pressure drawdown. However, this poses a practical difficulty. Oil production rates are proportional to the drawdown and by minimizing drawdown, one may avoid coning; but this would also result in reducing the oil production rate (Igbokoyi, 2011).

3.4.3   Reservoir and Well Model for a Constant Pressure Boundary System

If the reservoir has constant pressure boundaries (edge water, gas cap, bottom water), the pressure is equal to the initial value at such boundaries during production. With reference to figure 3.1, and assuming the partially completed well has a constant pressure boundary either at the bottom or the peripheral of the reservoir, the diffusivity equation is solved with the following boundary conditions.

The following assumptions are made in the derivation of the equation for the constant pressure boundary case.

1. At time t=0, the pressure is uniformly distributed in the reservoir, equal to the initial pressure P_i. The reservoir is with finite uniform thickness   h while the productive interval is h_p which spans across the completed interval.

2. The well is taken as a uniform line source, the drilled well length is h, the producing well length is h_p which spans across the completed interval and the wellbore radius is; r_w.

3. There is a single phase fluid, of small and constant compressibility, constant viscosity μ, and formation volume factor, which flows from the reservoir to the well. Fluid properties are not dependent on pressure and gravity and capillary forces are negligible.

4. There is no water encroachment or water/gas coning and multiphase flow effects are ignored.

5. If the reservoir is with top and bottom constant pressure boundaries, i.e., the boundaries at z=0 and z=h are both constant pressure boundaries, e.g. if the reservoir has both gas cap drive and bottom water drive, then:

$(P)_{z=0} = P_i$, and $(P)_{z=h} = P_i$

The radial form of the diffusivity equation used to derive the solution is presented below with its appropriate boundary conditions to suit a constant pressure boundary case.

Recall equations (3.1), (3.3) and (3.4) from closed boundary case;

$$\frac{\partial^2 P_D}{\partial r^2_D} + \frac{1}{r_D} \cdot \frac{\partial P_D}{\partial r_D} + \alpha \frac{\partial^2 P_D}{\partial z^2_D} = \frac{\partial P_D}{\partial t_D} \tag{3.1}$$

Inner boundary condition

$$C_D \frac{\partial P_{wD}}{d_{tD}} - \left(r_D \frac{\partial P_D}{\partial r_D} \right)_{r_D=1} \quad _{z_{D1} \leq z_D \leq z_{D2}} = 1 \tag{3.3}$$

$$P_{wD} = P_D - S \left(r_D \frac{\partial P_D}{\partial r_D} \right)_{r_D=1} \tag{3.4}$$

Outer B.C

$$P_D(r_{eD}, t_D) = 0 \qquad\qquad r_{eD} = \frac{r_e}{r_w} \qquad\qquad (3.8)$$

For this constant pressure boundary case, the solution to the partial differential equation is obtained by employing Laplace and Fourier Transformations with the appropriate boundary conditions. The dimensionless wellbore pressure obtained is as follows with skin and wellbore storage effects.

$$\bar{P}_{wD}$$

$$= \frac{\varphi}{C_D u^2 \omega} + \frac{1}{h_{fD}} \sum_{n=1}^{\infty} \frac{1}{n\pi u} \left(\frac{[\sin n\pi z_{D2} - \sin n\pi z_{D1}]\vartheta}{C_D u \beta} \right) cos(n\pi z_D) \qquad (3.9)$$

Where;

$$\varphi = K_0(r_{eD}\sqrt{u})I_0(\sqrt{u}) - K_0(\sqrt{u})I_0(r_{eD}\sqrt{u}) - S\sqrt{u}K_0(r_{eD}\sqrt{u})I_1(\sqrt{u}) - S\sqrt{u}K_1(\sqrt{u})I_0(r_{eD}\sqrt{u})$$

$$\omega = \left(K_0(r_{eD}\sqrt{u})I_0(\sqrt{u}) - K_0(\sqrt{u})I_0(r_{eD}\sqrt{u}) - S\sqrt{u}K_0(r_{eD}\sqrt{u})I_1(\sqrt{u}) - S\sqrt{u}K_1(\sqrt{u})I_0(r_{eD}\sqrt{u}) \right)$$
$$- \sqrt{u}K_0(r_{eD}\sqrt{u})I_1(\sqrt{u}) - \sqrt{u}I_0(r_{eD}\sqrt{u})K_1(\sqrt{u})$$

$$\vartheta = K_0(r_{eD}\sqrt{f})I_0(\sqrt{f}) - K_0(\sqrt{f})I_0(r_{eD}\sqrt{f}) - S\sqrt{f}K_0(r_{eD}\sqrt{f})I_1(\sqrt{f}) - S\sqrt{f}K_1(\sqrt{f})I_0(r_{eD}\sqrt{f})$$

$$\beta = \left(K_0(r_{eD}\sqrt{f})I_0(\sqrt{f}) - K_0(\sqrt{f})I_0(r_{eD}\sqrt{f}) - S\sqrt{f}K_0(r_{eD}\sqrt{f})I_1(\sqrt{f}) \right.$$
$$\left. - S\sqrt{f}K_1(\sqrt{f})I_0(r_{eD}\sqrt{f}) \right) - \sqrt{f}K_0(r_{eD}\sqrt{f})I_1(\sqrt{f}) - \sqrt{u}I_0(r_{eD}\sqrt{f})K_1(\sqrt{f})$$

$C_D \rightarrow 0 \; and \; S \rightarrow 0$, and leaves the above dimensionless pressure equation at the well without skin and wellbore storage effects as shown below:

$$\bar{P}_{wD}$$

$$= \frac{-1}{u^{\frac{3}{2}}} \left[\frac{K_0(r_{eD}\sqrt{u})I_0(\sqrt{u}) - K_0(\sqrt{u})I_0(r_{eD}\sqrt{u})}{K_0(r_{eD}\sqrt{u})I_1(\sqrt{u}) + I_0(r_{eD}\sqrt{u})K_1(\sqrt{u})} \right]$$

$$+ \frac{1}{hfD} \sum_{n=1}^{\infty} \frac{-1}{n\pi u} \left[\frac{(\sin n\pi z_{D2} - \sin n\pi z_{D1})K_0(r_{eD}\sqrt{f})I_0(\sqrt{f}) - K_0(\sqrt{f})I_0(r_{eD}\sqrt{f})}{\sqrt{f}K_0(r_{eD}\sqrt{f})I_1(\sqrt{f}) + \sqrt{f}I_0(r_{eD}\sqrt{f})K_1(\sqrt{f})} \right]$$

$$\times \cos(n\pi z_D) \qquad (3.10)$$

The parameters have the same meaning as in the case of the closed system.

The procedure for the derivation of the dimensionless well pressure is given under appendix A2.

The equation (3.9) can be programmed in MATlab with the application of Gaver-Stehfest algorithm (1970) for Laplace inversion; dimensionless pressure values with dimensionless time are generated which are used to obtain a pressure graph.

The graph depicts the pressure and pressure derivative versus time for a constant pressure

boundary case with partial completion at the centre of the vertical well with different well bore storage (C_De2S) and skin ($S_m=0.5Log\ (e2S)$) values.
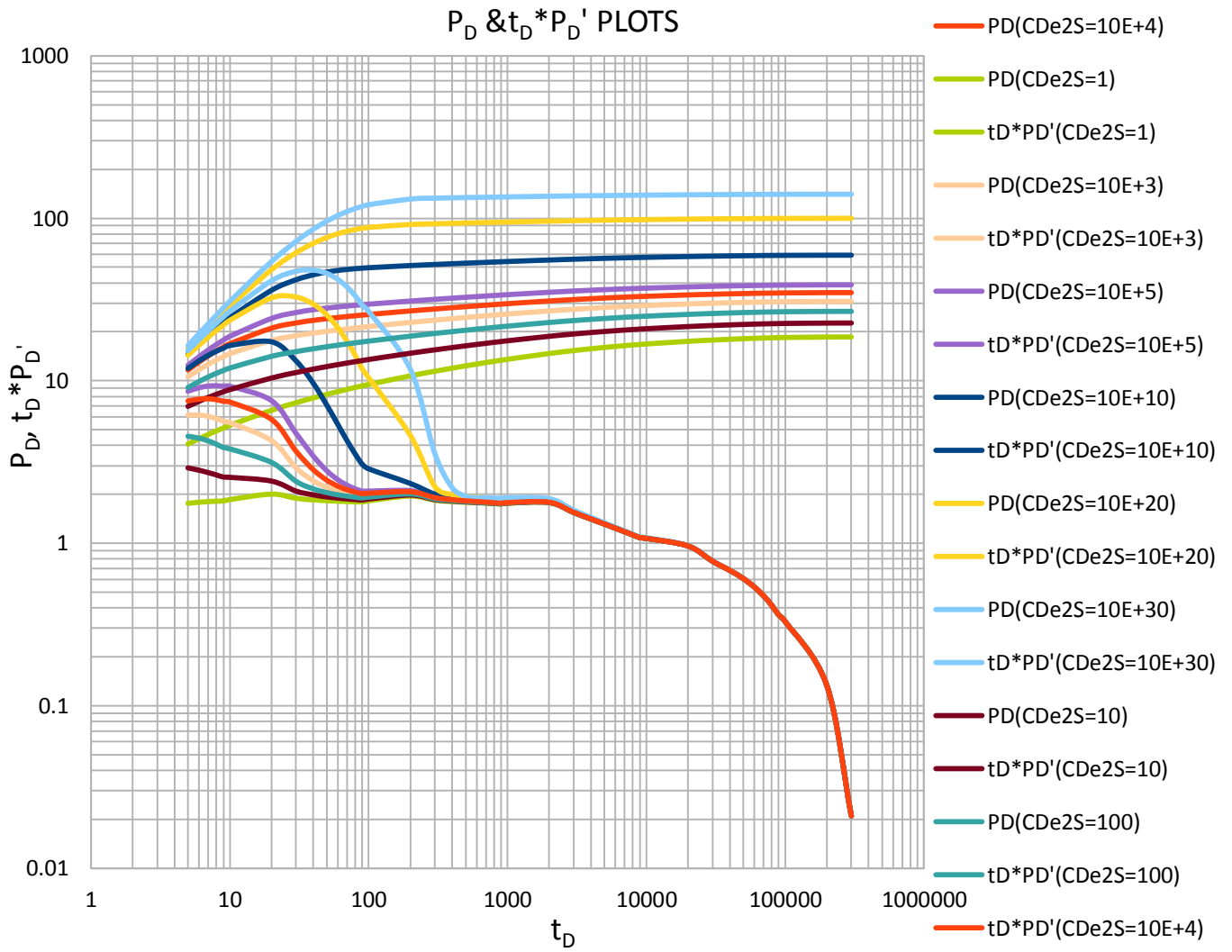
Figure 3.5 Pressure and Pressure Derivative curves depicting a constant pressure boundary

CHAPTER FOUR

PRODUCTIVITY INDEX AND SHAPE FACTOR FOR VERTICAL WELLS WITH PARTIAL COMPLETION

4.1   Productivity Index

Productivity index, PI is defined as the production rate per unit pressure drawdown. The transient productivity index is calculated before the flow reaches the pseudo-steady state or steady state regime. During the transient flow period, the efficiency with which a well is produced is defined in terms of its productivity index, PI, defined as:

$$PI = \frac{oil\ rate}{pressure\ drawdown} = \frac{q_0}{P_i - P_{wf}}$$
(4.1)

Where:

q_o is the oil flow rate

P_i is the initial reservoir pressure and

P_{wf} is the flowing bottom-hole pressure.

The larger the PI, the greater the oil rate for a given pressure drawdown and the smaller the number of wells required to develop the accumulation.

When a reservoir is bounded with a constant pressure boundary (such as a gas cap or an aquifer), flow reaches the steady state regime after the pressure transient reaches the constant pressure boundary. Rate and pressure become constant with time at all points in the reservoir and wellbore once steady state flow is established. Therefore, the productivity index during steady state flow is a constant, (Cheng, 2003).The expression for the productivity index is:

$$PI = \frac{oil\ rate}{pressure\ drawdown} = \frac{q_0}{P_e - P_{wf}}$$
(4.2)

Where:

P_e is the outer boundary pressure.

For a closed system reservoir with no-flow boundaries, flow enters the pseudo-steady state regime when the pressure effect reaches all boundaries after pressure drop for a long time. During this period, the rate at which pressure declines is almost the same at all points in the reservoir and at the wellbore.   Thus, average reservoir pressure is used instead of initial pressure when defining pseudo steady state productivity index. The difference between the average reservoir pressure and the well bore flowing pressure approaches a constant with respect to time. The pseudo steady state productivity index is normally constant.

The pseudo steady state productivity index is defined as:

$$PI = \frac{oil\ rate}{pressure\ drawdown} = \frac{q_0}{\bar{p}_R - P_{wf}}$$

(4.3)

Where:

$\bar{p}_R$ is the average reservoir pressure.

4.2   Shape Factors

Shape factors are correction factors which are designed to account for the deviation of the drainage area of a well from the ideal circular form.

The effect of the shape of the drainage area surrounding a well and the location of the well within the specified drainage area is reflected in terms of the shape factor C_A. The value of C_A is high for shapes of large values of the ratio of the area to the perimeter, and for centrally located well. While the value of shape factor is low for offset well locations and for drainage shapes of small area to perimeter ratios (Noaman, 1982).

Shape factor can be seen to be dependent not only on the drainage shape but also upon the position of the well with respect to the boundary. Dietz (1965) came up with shape factor values which depict a particular well position in regular reservoir configurations (shapes). For irregular shapes, interpolation between these geometrical configurations presented by Dietz may be necessary.

Naturally it is never possible to obtain the exact shape of the drainage volume but a reasonable estimate can usually be made which, when interpreted in terms of a shape factor and used, can considerably improve the accuracy of calculations made using pressure drop equation and consequently, the productivity index.

The magnitude of shape factor depends on the shape of the area being drained and also upon the position of the well with respect to the boundary.

4.3   ESTIMATION OF AVERAGE RESERVOIR PRESSURE

Average reservoir pressure $\bar{P}_R$, can be determined from a pressure buildup test. Also, $\bar{P}_R$ is referred to as static drainage area pressure in the formation surrounding a tested well. Average reservoir pressure is used:

1. To compute rock and fluid characteristics.

2. To estimate oil in-place.

3. To predict future reservoir behaviour in primary/secondary recovery and pressure maintenance projects.

Note that initial or original reservoir pressure is different from average reservoir pressure. Average reservoir pressure is determined for reservoirs that have experienced some pressure depletion. Several methods are available to estimate average reservoir pressure.

In order to assess the productivity of a reservoir, the late time state of the reservoir is used, that is, the pseudo-steady state. Equations for calculation of the productivity index in this study have been generated for various reservoir cases namely; the closed system, bottom water and peripheral water. The procedures for obtaining such equations are outlined under the different reservoir type cases.

4.4   General Solution to Productivity Index Equations

In all the three cases, the following were employed:

The source functions are obtained from Gringarten and Ramey (1973) which depict the particular reservoir type in question.

Employing Babu and Odeh's approach used for horizontal well, the source functions are integrated twice along the vertical direction of the well and also time, τ, Carslaw and Jaeger (1959) have shown that τ is time in order to obtain a line sink solution as seen in the following expression;

$$\Delta P = P_i - P(x, y, z, t) = \left[\frac{886.9B\mu q}{abhL\alpha}\right] \int_0^t \int_{z_1}^{z_2} (S_1.S_2.S_3) \, dz_o d_\tau \tag{4.4}$$

With

$$\alpha = 157.952\emptyset\mu C_t \ days \tag{4.5}$$

$$L = (z_2 - z_1) \rightarrow lenght \ of \ completion \ interval \ of \ vertical \ well, ft \tag{4.6}$$

Parameters: a, b and h are distances in the x, y and z directions respectively, and for an anisotropy case, a, b and h are not equal and also, $k_x \neq k_y$; $x_o, y_o, \ and \ z_o$ are respectively the well positions in the x, y and z directions.

The reservoir is considered to be of a rectangular shape with the well at its centre.
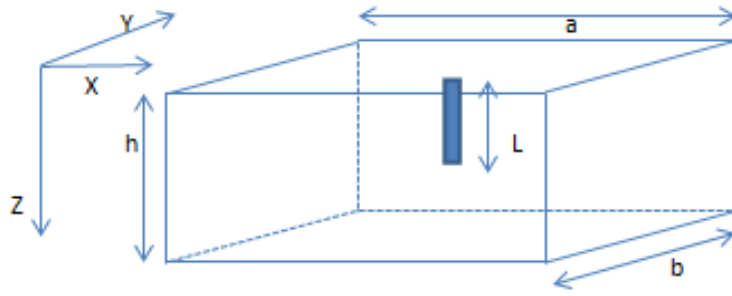
Figure 4.1 Schematic illustrating the reservoir and well model.

4.5   WORK PROCEDURE

The productivity index equations were obtained by integrating the appropriate point source functions obtained from Gringarten and Ramey along the correct parameters to obtain a line sink solution.

The equations are thus programmed in MATlab and using the values of the parameters given in table 4.1, pressure drop and productivity index are obtained.

For a comparative analysis, the equations are programmed such that, the productive/completed interval are varied and their corresponding productivity indices and pressure drops are obtained.

4.5.1   Productivity Index Equation for Closed Boundary System

The following point source functions depicting a no-flow boundary case from Gringarten and Ramey are used.

$$S_1 = S_1(x, x_o, \tau) = 1 + 2 \sum_{n=1}^{\infty} \cos \frac{n\pi x}{a} \cos \frac{n\pi x_o}{a} exp \left[-\frac{n^2 \pi^2 k_x \tau}{\alpha a^2} \right] \tag{4.7}$$

$$S_2 = S_2(y, y_o, \tau) = 1 + 2 \sum_{m=1}^{\infty} \cos \frac{m\pi y}{b} \cos \frac{m\pi y_o}{b} exp \left[-\frac{m^2 \pi^2 k_y \tau}{\alpha b^2} \right] \tag{4.8}$$

$$S_3 = S_3(z, z_o, \tau) = 1 + 2 \sum_{l=1}^{\infty} \cos \frac{l\pi z}{h} \cos \frac{l\pi z_o}{h} exp \left[-\frac{l^2 \pi^2 k_z \tau}{\alpha h^2} \right] \tag{4.9}$$
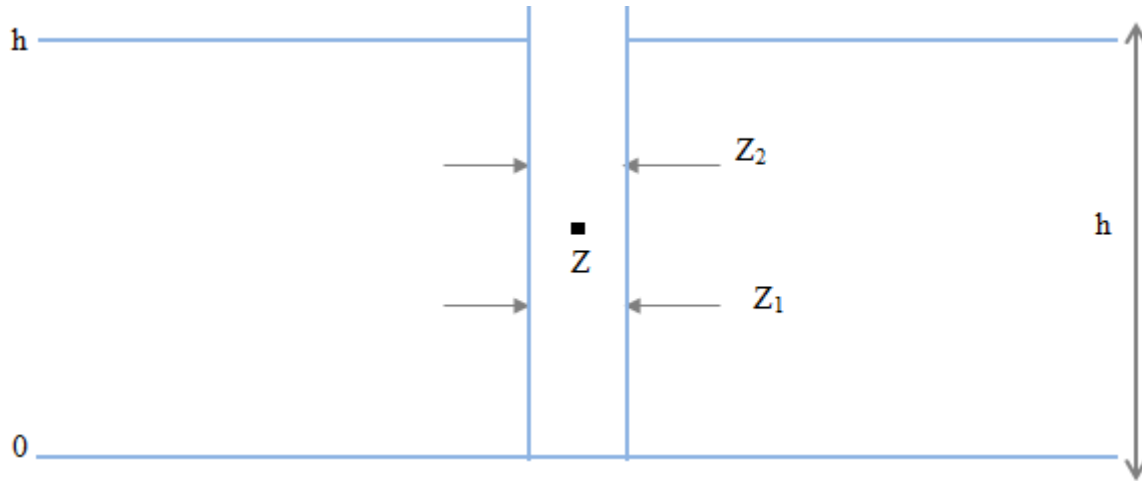
Figure 4.2 Schematic for Closed system

The entire procedure in the derivation of the productivity index is given in appendix B1. For a closed system reservoir the productivity index equation for a partial completion case can be deduced from the pressure drop equation as:

$$\overline{\Delta P} = \left[\frac{141.15 B \mu q}{h\sqrt{k_x k_y}}\right][P_x + P_y + P_z + P_{xy} + P_{xz} + P_{yz} + P_{xyz}] \qquad (4.10)$$

$$J = \frac{q_o}{\Delta P} = \frac{h\sqrt{k_x k_y}}{141.15 B \mu (P_x + P_y + P_{xy})} \qquad (4.11)$$

Equation (4.11) is the productivity index for full completion case.

Where Px, Py, Pz, Pxy, Pxz, Pyz, Pxyz are given in appendix B1

The pressure drop for a 3-D partial completion in vertical well in closed system can be further expressed as:

$$\overline{\Delta P} = \frac{141.2 q \mu B}{h\sqrt{k_x k_y}}\left[ln\left(\frac{r_w \sqrt{A}\, exp(0.75 + P_x + P_y + P_{xy})_{wellbore}}{r_w \sqrt{A}\, exp(0.75)}\right) + S_R + S_m\right] \qquad (4.12)$$

$$\overline{\Delta P} = \frac{141.2 q \mu B}{h\sqrt{k_x k_y}}\left[ln\left(\frac{\sqrt{A}}{r_w} C_A\right) - 0.75 + S_R + S_m\right] \qquad (4.13)$$

Where, C_A is a shape factor.

S_R is the skin factor due to partial completion and S_m is the damaged skin factor.

The productivity index equation with skin and shape factor can be rearranged as:

$$PI = \frac{h\sqrt{k_x k_y}}{141.2 q \mu B\left[ln\left(\frac{\sqrt{A}}{r_w} C_A\right) - 0.75 + S_R + S_m\right]} \qquad (4.14)$$

For a full completion case:

$$PI = \frac{h\sqrt{k_x k_y}}{141.2q\mu B \left[ln\left(\frac{\sqrt{A}}{r_w} C_A \right) - 0.75 + S_m \right]}$$

(4.15)

4.5.1.1 Application of Closed System PI Model

The reservoir fluid and well properties used for the generation of the productivity index are given below

Table 4.1: Reservoir, Well and Fluid Property values

Parameter	Value
Pay zone thickness (h)	100 ft.
Completion Length (L_p)	10 – 100 ft.
Permeability in x direction (K_x)	100mD
Permeability in y direction (K_y)	400mD
Permeability in z direction (K_z)	25mD
Flow rate (q)	4746 STB/D
Formation volume factor (B_o)	1.38rb/stb
Oil viscosity (μ_o)	0.422 cp
Distance of well in x direction (a)	4000 ft.
Distance of well in y direction (b)	2000 ft.
Well bore position in x direction (x_o)	2000 ft.
Well bore position in y direction (y_o)	1000 ft.
Well bore position in z direction ($z_o = \frac{z_1+z_2}{2}$)	

The table below gives the results obtained for closed system PI model.

Table 4.2: Closed system Productivity Index and ΔP Results

Penetration ratio	ΔP(Partial completion)	ΔP(full completion)	J(partial)	J(full)
0.1	509.0735	129.7292	9.3228	36.5839
0.2	337.1978	129.7292	14.0748	36.5839
0.3	262.1894	129.7292	18.1014	36.5839
0.4	219.4096	129.7292	21.6308	36.5839
0.5	191.5374	129.7292	24.7784	36.5839

0.6	171.8648	129.7292	27.6147	36.5839
0.7	157.227	129.7292	30.1857	36.5839
0.8	145.9245	129.7292	32.5237	36.5839
0.9	136.9644	129.7292	34.6513	36.5839
1	129.7292	129.7292	36.5839	36.5839

The plots of the productivity index (J) and pressure drop (ΔP) versus completion interval (L_p) are as shown below:
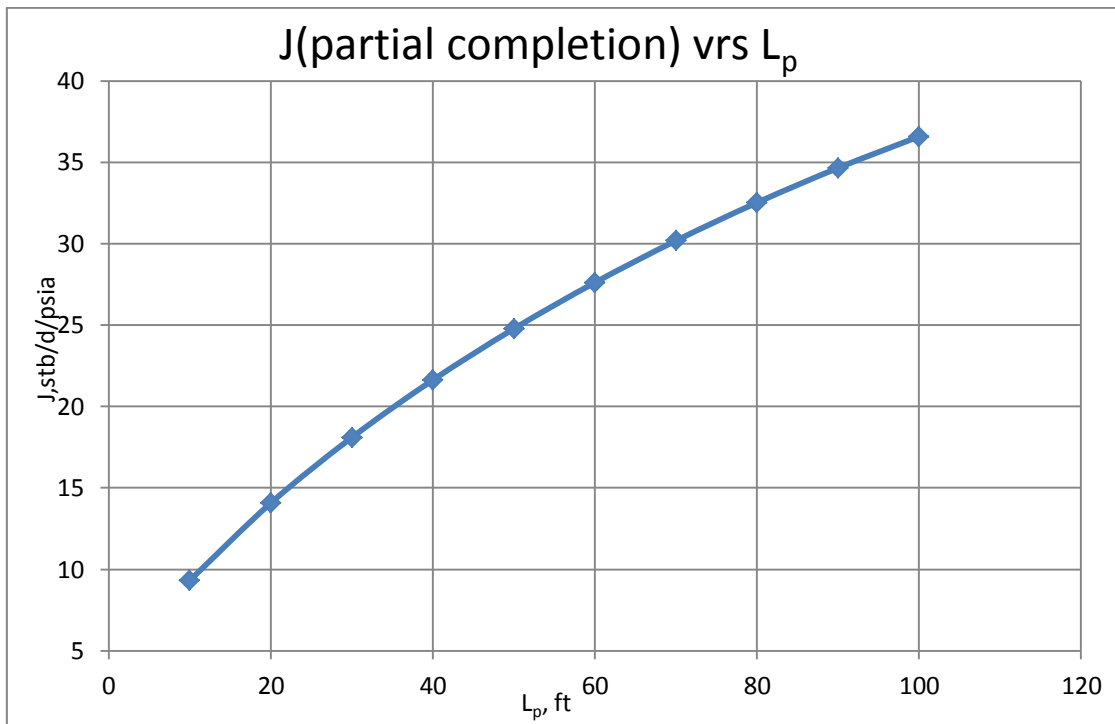
Figure 4.3 Productivity index versus completion length
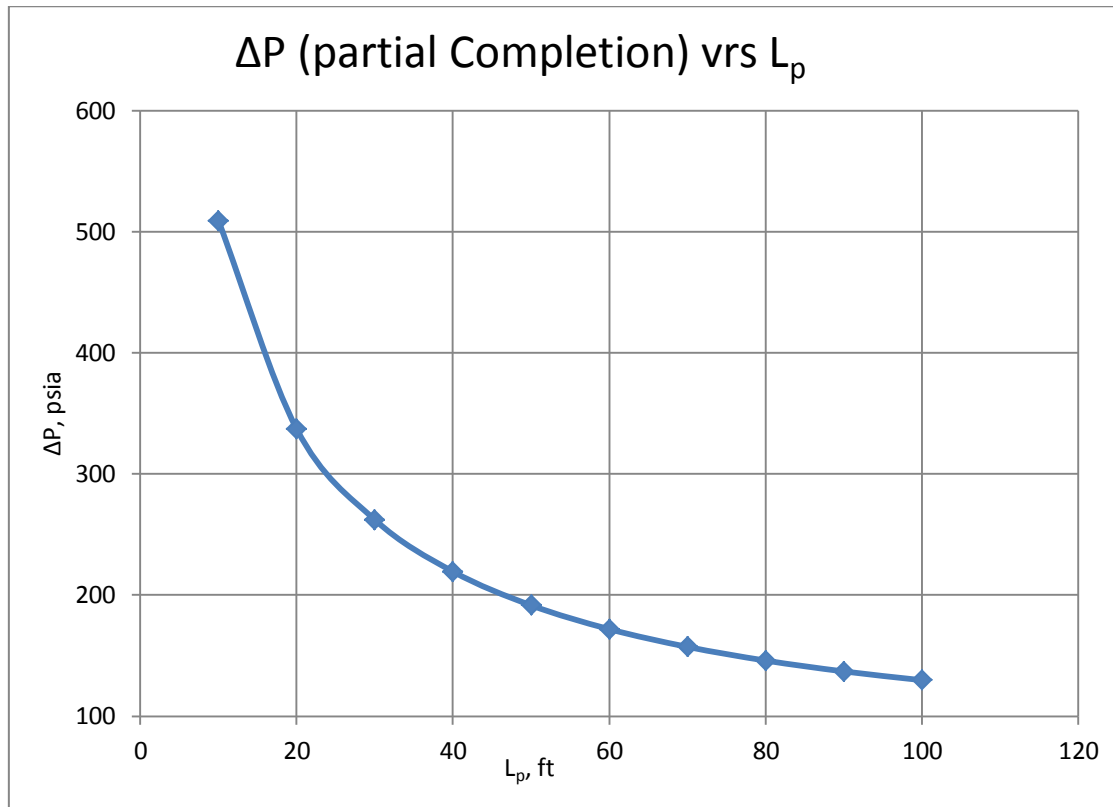
Figure 4.4 Pressure Drop versus Completion Length

4.5.2. Productivity Index Equation for Constant Pressure Boundary System

Case 1: Bottom water system

The flowing source functions from Gringarten and Ramey are used:

Recall equations (4.7) and (4.8) from the closed system case;

$$S_1 = S_1(x, x_o, \tau) = 1 + 2 \sum_{n=1}^{\infty} \cos\frac{n\pi x}{a} \cos\frac{n\pi x_o}{a} \, exp\left[-\frac{n^2\pi^2 k_x \tau}{\alpha a^2}\right] \qquad (4.7)$$

$$S_2 = S_2(y, y_o, \tau) = 1 + 2 \sum_{m=1}^{\infty} \cos\frac{m\pi y}{b} \cos\frac{m\pi y_o}{b} \, exp\left[-\frac{m^2\pi^2 k_y \tau}{\alpha b^2}\right] \qquad (4.8)$$

$$S_3 = \sum_{l=1}^{\infty} \cos(2l+1)\frac{\pi z_0}{h} \cos(2l+1)\frac{\pi z}{h} \, exp\left[-\frac{(2l+1)^2\pi^2 k_z \tau}{4\alpha h^2}\right] \qquad (4.16)$$

The entire procedure in the derivation of the productivity index is given in appendix B2. For bottom water system, the productivity index can be calculated from the pressure drop equation as:

$$\overline{\Delta P} = (\bar{P}_R - P) = \left[\frac{886.9 B\mu q}{abhL}\right]\left[P_z + P_{xz} + P_{yz} + P_{xyz}\right] \tag{4.17}$$

Where P_z, P_{xz}, P_{yz}, P_{xyz} are given under appendix B2.

4.5.2.1 Application of Case 1 PI Model

With the application of the data given in table 4.1 a normalized productivity index has been obtained. Pressure drops recorded were very small leading to high productivity values.

The normalised productivity index involves the productivity ratio of the partial completion to that of full completion. Figure 4.4 depicts the trend for the normalized productivity ratio plotted with penetration ratios of the well.
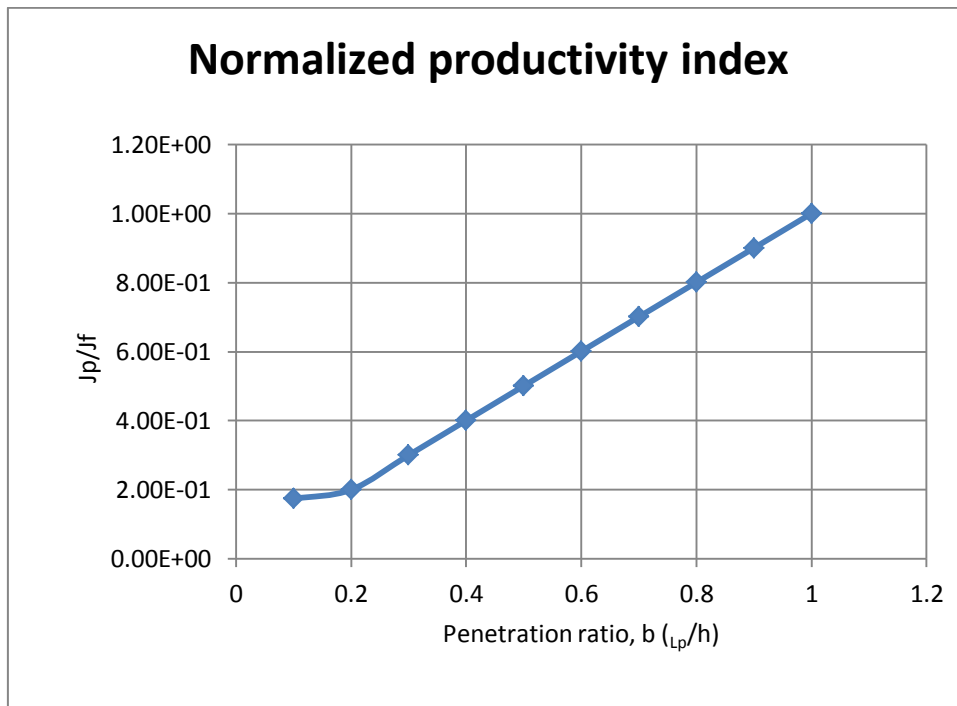
Figure 4.5 Normalised PI versus penetration ratio

Case 2: Peripheral System (bottom and edge water)

From Gringarten and Ramey the following point source functions are used in the derivation of the productivity equation. Recall S_3 from equation (4.16);

$$S_1 = \sum_{n=1}^{\infty} \cos(2n+1)\frac{\pi x_0}{a}\cos(2n+1)\frac{\pi x}{a}exp\left[-\frac{(2n+1)^2\pi^2 k_x \tau}{4\alpha a^2}\right] \tag{4.18}$$

$$S_2 = \sum_{m=1}^{\infty} \cos(2m+1)\frac{\pi y_0}{b}\cos(2m+1)\frac{\pi y}{b}exp\left[-\frac{(2m+1)^2\pi^2 y\tau}{4\alpha b^2}\right] \tag{4.19}$$

$$S_3 = \sum_{l=1}^{\infty} \cos(2l+1)\frac{\pi z_0}{h}\cos(2l+1)\frac{\pi z}{h}exp\left[-\frac{(2l+1)^2\pi^2 k_z\tau}{4\alpha h^2}\right] \tag{4.16}$$

The entire procedure in the derivation of the productivity index is also given under appendix B3. The productivity index can be calculated from the pressure drop equation as:

$$\overline{\Delta P} =$$

$$\left[\frac{886.9B\mu q}{abh(z_2-z_1)}\right]\frac{4h}{\pi^3}\sum_{n,m,l}^{\infty}\frac{\cos(2n+1)\frac{\pi x}{a}\cos(2n+1)\frac{\pi x_0}{a}\cos(2n+1)\frac{\pi y}{b}\cos(2n+1)\frac{\pi xy_0}{b}\cos(2l+1)\frac{\pi z}{h}\left[\sin\frac{(2l+1)\pi z_2}{h}-\sin\frac{(2l+1)\pi z_1}{h}\right]}{(2l+1)\left[\frac{(2n+1)^2 k_x}{a^2}+\frac{(2m+1)^2 k_y}{b^2}+\frac{(2l+1)^2 k_z}{h^2}\right]} \tag{4.20}$$

Where, MATlab program is used to evaluate this.

4.6   SHAPE FACTOR C_A AND PSEUDO-SKIN

For anisotropic cases, Babu and Odeh (1989) obtained certain equations for their horizontal well. They came up equations for pseudo skin and shape factor as in the following respectively.

$$S_R = \left(P_y + P_{xy} + P_{yz} + P_{xyz}\right)_{WB} \tag{4.21}$$

$$lnC_H + ln\left(\frac{\sqrt{ab}}{r_w}\right) - 0.75 = (P_x + P_z + P_{xz})_{WB} \tag{4.22}$$

From equation (4.9), in terms of the shape factor, the terms $[P_x+P_y+P_{xy}]$ represent the 2D effects of a full penetration case. The other terms $[P_z+P_{xz}+P_{yz}+P_{xyz})$ are identified with skin due to partial completion.

Therefore equations for skin due to partial completion and shape factor for vertical well case are given respectively as:

$$S_R = \left(P_z + P_{xz} + P_{yz} + P_{xyz}\right)_{WB} \tag{4.23}$$

And

$$lnC_A + ln\left(\frac{2.2459A}{r_w}\right) - 2\left(P_x + P_y + P_{xy}\right)_{WB} \tag{4.24}$$

For fully penetrating and completion S_R is zero. Therefore,

$$ln\left[exp\left(P_x + P_y + P_{xy}\right)_{wellbore}\right] = \frac{1}{2}ln\left(\frac{4A}{r_w^2\gamma C_A}\right) \tag{4.25}$$

Expanding equation (4.25) and making CA subject of the formula will yields the general formulae

for the calculation of the shape factors as:

$$ln C_A = ln\left(\frac{2.2459A}{r_w}\right) - 2\left(P_x + P_y + P_{xy}\right)_{wellbore} \qquad (4.26)$$

Equation (4.26) is used to compute the three dimensional shape factors in a closed system equivalent to Dietz shape factor.

Where,

r_w is the wellbore radius,

A is the drainage area of the wellbore and

γ is the Euler's exponential constant

C_A represents the shape factor of the vertical wellbore.

P_x, P_y, P_z, P_{xy}, P_{zy}, P_{xz} and P_{xyz} are given under Appendix A1.

4.6.1 New Shape Factor

From equation (4.12), a new shape factor equation has been derived for vertical wells.

$$C_A = \frac{r_w exp\left(0.75 + P_x + P_y + P_{xy}\right)_{wellbore}}{\sqrt{A}} \qquad (4.27)$$

$$C_A = 2.117 \frac{r_w exp\left(P_x + P_y + P_{xy}\right)_{wellbore}}{\sqrt{A}} \qquad (4.28)$$
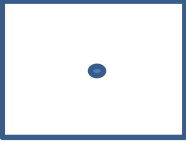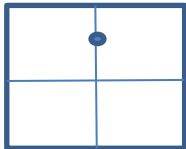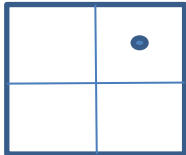
Equation (4.28) gives an expression similar to that of Babu and Odeh for horizontal wells in a rectangular system. Knowing the rectangular area $ab - ft^2$ of the horizontal plane, well position, C_A can be estimated.

4.7 A COMPARATIVE ANALYSIS WITH DIETZ SHAPE FACTORS

Equations (4.26) and (4.28) have been employed to calculate shape factors for bounded reservoirs using the same configurations employed by Dietz. The results are presented below:

Table 4.3: Shape Factors (comparison with Dietz shape factors (1965))

Bounded reservoirs	lnC_A : Dietz Shape Factors (Expected)	lnC_A Obtained for equation (4.28)	lnC_A Obtained for equation (4.26)

	3.43	3.4465	4.8385
	2.56	2.6216	4.1379
	1.52	2.6215	2.4879
	3.12	3.13	3.13
	-1.46	3.4706	-0.5198
	0.86	5.6788	-1.9765
	1.168	5.0432	-6.803

CHAPTER FIVE

FACTORS AND PARAMETERS THAT INFLUENCE/CONTROL PI

5.1   INTRODUCTION

Several factors and parameters have been identified to greatly influence PI values. These parameters are vertical permeability, pseudo skin, well position, drainage area and etc. These have been analysed and their results show the extent of influence they have on productivity index values.

5.2   EFFECTS OF PSEUDO-SKIN ON PRODUCTIVITY INDEX

Compared to an open-hole or fully completed vertical well, the additional pressure loss/gain caused by the different perforations intervals may be considered as a pseudo skin factor. The well with L_p perforation interval produces at a constant flow rate. The formation is sealed at the top and bottom as well as the well peripheral. The well communicates with the reservoir only through the perforations.

Equation (4.23) has been used to calculate the additional pressure drop due to partial completion and the associated productivity index. . In equation (4.23), S_R is the skin factor due to partial completion and it is estimated with the expressions for P_z, P_{xz}, P_{yz} and P_{xyz}. The skin factor is determined from a pressure transient analysis.

Table 5.1: Results for Pseudo skin and Productivity Index

Penetration Ratio (L_p/h)	ΔP (Partial completion)	J (partial completion)	Pseudo-skin (S_R)
0.1	509.0735	9.3228	19.4475
0.2	337.1978	14.0748	10.6361
0.3	262.1894	18.1014	6.7907
0.4	219.4096	21.6308	4.5976
0.5	191.5374	24.7784	3.1687
0.6	171.8648	27.6147	2.1601
0.7	157.227	30.1857	1.4097
0.8	145.9245	32.5237	0.8303

0.9	136.9644	34.6513	0.3709
1	129.7292	36.5839	0

Below is a plot showing pseudo skin versus perforation/completion interval.
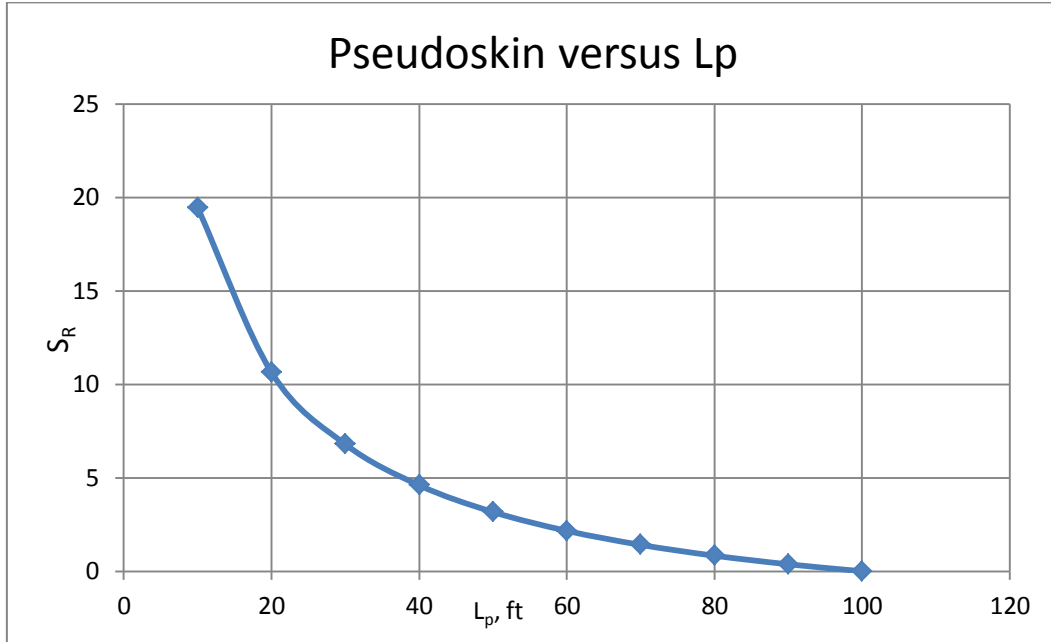
Figure 5.1 Relationship between Pseudo skin and Completion Interval

5.3   EFFECTS OF GEOMETRIC SHAPE FACTOR ON PRODUCTIVITY INDEX

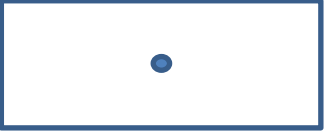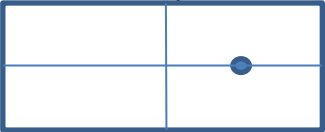In chapter four, it was found that equation (4.28) gives results similar to that of Babu and Odeh for horizontal wells in a rectangular system. Knowing the rectangular area $ab - ft^2$ of the horizontal plane, well position, C_A can be estimated from Table 5.2.

Shape factors are obtained for different well positions within the reservoir drainage area. Figure 5.2 illustrates a grid rectangular drainage area of the reservoir and also shows different well positions whose shape factors have been calculated.

This analysis has been carried out by employing equations (4.28) and (4.15) for the calculation of shape factors and the associated productivity index respectively.

42
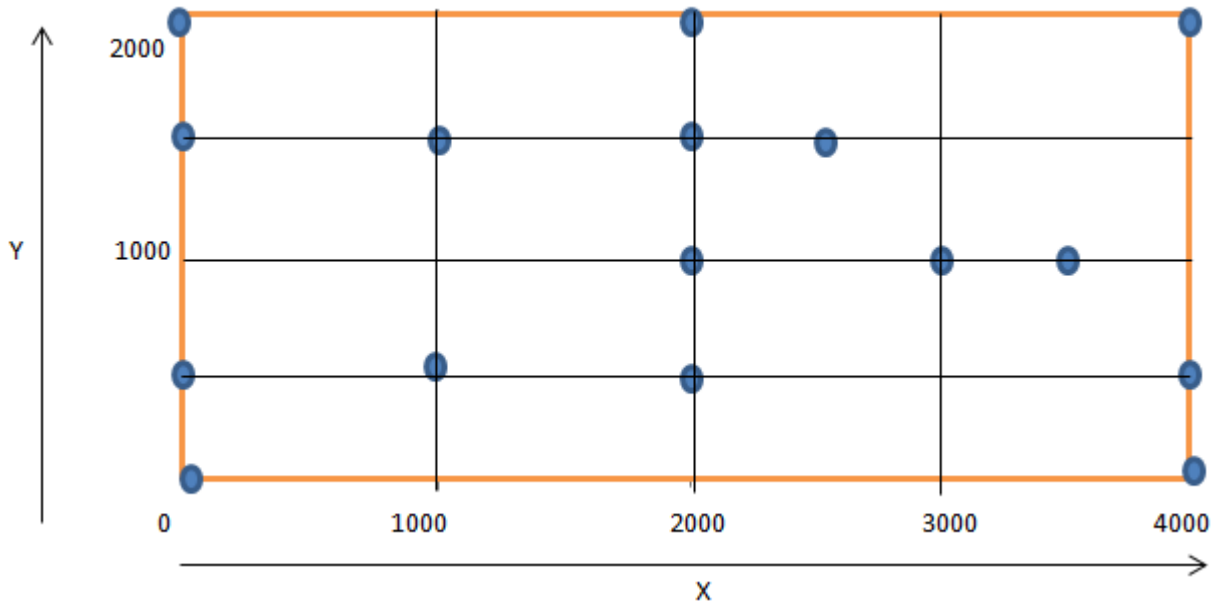
Figure 5.2 Reservoir Drainage Area showing different Well Positions

Table 5.2: Results for Wells within and around the centre of Reservoir Drainage Area

Position (X_o to Y_o)	J	Shape Factors C_A	lnC_A
2000/1000	20.9319	22.737	3.124
2000/1750	19.3336	59.4154	4.0845
3750/1000	14.7636	2.92E+03	7.9793
2000/1500	20.3256	32.1552	3.4706
3000/1000	18.4392	109.3763	4.6948
3000/1500	17.9646	154.97	5.0432
3500/1000	16.0481	780.672	6.6602
1000/500	17.9646	154.97	5.0432
1000/1500	17.9646	154.97	5.0432

5.4 EFFECT OF PERMEABILITY ON PRODUCTIVITY INDEX (PI)

Analysis on the effect of vertical to horizontal permeability ratio on productivity index has been carried out, and the result shows a clear dependency of productivity on vertical permeability though a weak one. Equations (4.9) and (4.23) have been employed.

Table 5.3: Results of Permeability ratio and Productivity Index

k_h=400mD				
$\frac{k_z}{k_h}$ (ratio)	k_z	ΔP(Psia)	J(STB/D/PSI)	S_R
0.1	40	93.8737	50.5573	3.4805
0.2	80	90.8802	52.2226	3.1736
0.3	120	89.0756	53.2806	2.9886
0.4	160	87.7761	54.0694	2.8553
0.5	200	86.7586	54.7035	2.751
0.6	240	85.9218	55.2363	2.6652
0.7	280	85.2107	55.6972	2.5923
0.8	320	84.5924	56.1044	2.5289
0.9	360	84.0452	56.4696	2.4728
1	400	83.5544	56.8013	2.4225
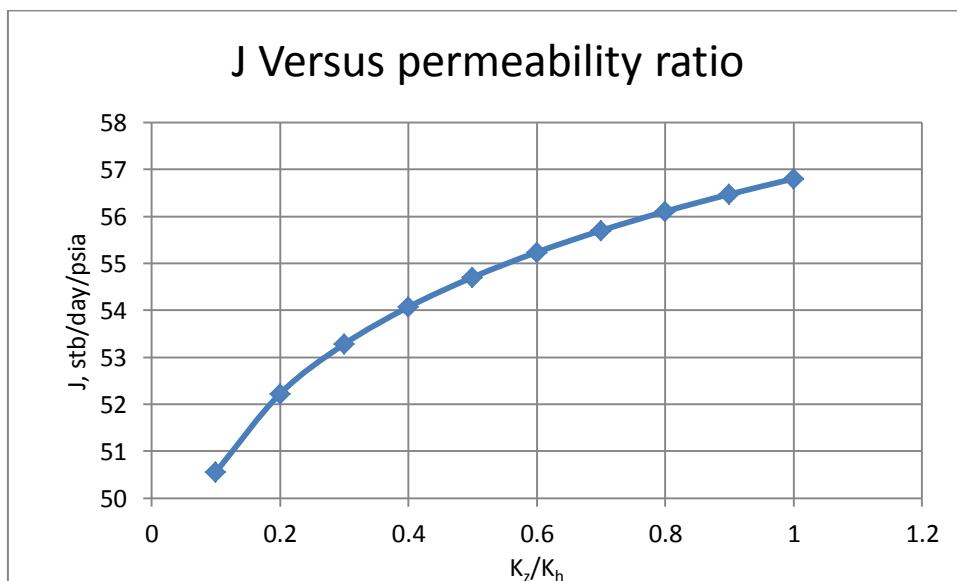
Figure 5.3 Relationship between PI and Permeability ratio

5.5 EFFECT OF RESERVOIR AREA EXTENT ON PRODUCTIVITY INDEX

Various area extents (large and small) have been used to observe whether they have any influence on productivity index. This analysis was carried out considering a fully completed well case and also a partially completed well with penetration ratio of 0.5. From the results, it is observed that, large areas contribute less to pressure drop whiles relatively smaller areas give large pressure drops.

Table 5.4: Results of Reservoir Drainage Area, Pressure Drop and Productivity Index

Area (A)×10^4 (ft^2)	ΔP (Partial completion)	ΔP (full completion)	J (L$_p$/h=0.5)	J (full)
16	233.623	158.5959	20.3148	29.9251
50	210.5647	129.7292	22.5394	36.5839
200	202.3052	129.7292	23.4596	36.5839
800	191.5374	129.7292	24.7784	36.5839
1500	183.5672	125.8708	25.8543	37.7053
2400	178.3039	124.1206	26.6175	38.237
3500	174.3067	123.139	27.2279	38.5418
4800	171.0557	122.5164	27.7454	38.7377

DISCUSSION OF RESULTS

For both closed system case and Bottom water, from figures 4.3 and table 4.5, it is evident that productivity index increases with increasing penetration ratio. From figure 4.3, it is observed that as penetration ratio increases, there is a decrease in pressure drop and the opposite occurs when penetration ratio is decreasing.

On the normalised productivity index for bottom water case as shown in figure 4.5, it is observed that the plot of productivity ratio versus penetration ratio depict a positive slope, which indicates that, J ratio increases proportionally with increasing penetration ratio. It further reveals that the higher the completion length, the higher the productivity index.

A number of factors which directly or indirectly affect productivity index have been examined such as: penetration ratio (completion length), permeability ratio, reservoir area, well position (shape factors) and skin due to restricted entry to flow. It is realized that all these factors have their influence contributing to high or low productivity.

Pseudo skin as a result of partial completion has been analysed by varying penetration ratio. Pseudo skin contributes to excess pressure drop leading to a decrease in productivity index. It is observed from figure 5.1 that as completion/perforation interval decreases there is a rise in pseudo skin values. It can be concluded that, any small restriction of flow caused by the perforation/completion interval has a positive skin associated with it but for an open-hole or a fully completed interval of perforation, there is no associated pseudo skin.

The effect of permeability ratio on productivity index gives a positive slope curve in figure 5.3. It is established from the graph that productivity index is directly proportional to permeability ratio. Whereas a high permeability ratio enhances productivity, a low permeability ratio leads to low productivity index.

Babu and Odeh (1989) carried out the same analysis for horizontal wells and came up with the view that, a decrease in vertical permeability by a factor of 4 decreases productivity index (J) by a factor of 1.8 for a fully penetrated well, and by a factor of 1.7 for a well with penetration ratio of 0.5.

In a nut shell, one can conclusively remark that, vertical permeability varies proportionally with productivity index. Also the results (Table 5.3) show that vertical permeability has an effect on skin although a weak one.

Additionally, it has been ascertained that, well positions affect productivity through the shape factors. The optimum position to place a well is at the centre of the drainage area since its effects on productivity loss is minimal. More so, the maximum effect of shape factor occurs when skin due to partial completion is zero (fully completed well) and pressure drop is minimum as presented in table 5.2. On the other hand, off-centred wells and wells placed at the borders of the drainage area have very high shape factors. They also contribute most to pressure drops and consequently leading to high productivity loss.

From table 5.4, one can observe a larger area extent leading to high productivity and relatively, small area extent giving out relatively low values of productivity index. However, the issue of area extent on productivity is relative because it would largely depend on the number of wells drilled within such an area and also the well position but from this study and considering a single well reservoir, it can clearly be stated that large area extent contribute to high productivity index relative to small area extent. For off-centred well, pressure drop was equally high as compared to centrally positioned wells.

Finally, new shape factors have been obtained for vertical wells from equation (4.28) which is similar to Babu and Odeh's (1989) for horizontal wells. Equation (4.26) (equivalent to Dietz's shape factors formulae) for different reservoir configurations as proposed by Dietz (1965) has also been used to calculate shape factors which gave close values for some of the reservoir shapes as compared to Dietz shape factors. The results, though not exact has been tabulated (table 4.3). The reason for the difference is the limitation to test the equations with real field data and also, the computation in the summations is not too stable. The essence of this analysis helps one to predict the shape factor of a particular well bore configuration and how much they contribute to productivity index gain or loss.

CHAPTER SEVEN

CONCLUSIONS AND RECOMMENDATIONS

7.1   CONCLUSIONS

1. An analytical model of evaluating productivity index in vertical wells which accounts for the effect of pressure drop due to partial completion has been obtained.

2. For a partially completed vertical well, PI is strongly controlled by the producing length, and weakly controlled by pay zone thickness, vertical permeability, well position and reservoir size.

3. For fully penetrated/completed wells, PI is strongly influenced by the well position through the shape factors.

7.2   RECOMMENDATIONS

1. Field data should be used to test the models in order to ascertain their validity

2. Different productivity equations should be used under different reservoir geometries as well as different boundary conditions.

3. The new shape factor equation (4.28) should be used for wells in rectangular shape reservoirs.

4. The analytical models can be further approximated for easy computation.

NOMENCLATURE

Symbol	Description	Units
q_o	Oil rate	stb/d
PI	Productivity Index	stb/d/psi
L_p	Completion well length	ft
S_R	Skin due to Partial completion	
h	Formation thickness	ft
K_x	Permeability in x direction	mD
K_y	Permeability in y direction	mD
K_z	Permeability in z direction	mD
K_h	Horizontal Permeability	mD
J	Productivity Index	stb/d/psi
a	Length of reservoir	ft
b	Width of reservoir	ft
P_R	Average reservoir Pressure	Psi

REFERENCES

Ahmed, T.: "Advanced Reservoir Engineering", 3rd Edition, 2005. Anadarko Petroleum Corporation.

Babu, D. K. and Odeh, A. S.: "Productivity of a Horizontal Well". SPE Reservoir Engineering, Vol.4, No.4, 417- 421, (Nov, 1989).

Bilhartz, H.L. Jr. and Ramey, H. J. Jr: "The Combined Effect of Storage, Skin and Partial Penetration on Well Test Analysis," paper SPE 6453 presented at the SPE 52nd Annual Technical Conference and Exhibition, Denver, Oct, 9-12, 1977.

Brons, F. and Martings, V. E.: "The Effect of Restricted Fluid Entry on Well Productivity". Journal of Petroleum Technology, 172-174, (February, 1961).

Carslaw, H. S., and Jaegar, J. C.: "*Conduction of Heat in Solids*," Oxford at the Clarendon Press, 1959, 2nd Edition, pp. 185.

Cheng, Y. M.: "Pressure Transient Testing and Productivity Analysis for Horizontal Wells", PhD Dissertation, Department of Petroleum Engineering, Texas A& M University, 2003.

Clegg, M. W. and Mills M.: "A study behavior of Partial Penetrated Wells", July, 1969

Craft, B. C. and Hawkins, M. F.: "Applied petroleum Reservoir Engineering", 2nd Edition, 1991.

Dake, L. P.: "Fundamentals of reservoir" Elsevier, 1978

Dietz, D. N.: "Determination of Average Reservoir Pressure from Build-Up Surveys". J. Pet. Tech., August, 1965.

Earlougher, R. C., Jr., Ramey, H. J., Jr., Miller, F. G., and Mueller, T. D.: "Pressure Distributions in Rectangular Reservoir". Journal of Petroleum Technology, 199-208, (February, 1968).

Economides, M.: *Petroleum production systems*, 1993

Gringarten, A. C., and Ramey, H. J., Jr.: "The use of Source and Green's functions in Solving Unsteady Flow Problems in Reservoirs," *Soc. Pet. Eng*. J. (Oct. 1973) 285-296; Trans., AIME, Vol. 255.

GRINGARTEN, A. C. and RAMEY, JR., H.J.: "An Approximate Infinite Conductivity Solution for a Partially Penetrating Line-Source Well". SPE Journal, Vol. 15, No.2, pp. 140-148, April 1975.

Horne, R. N.: "Modern Well Test Analysis, A computer Aided Approach", 1990

Igbokoyi, A. O.: "Horizontal Well Technology", Lecture material delivered at the African University of Science and Technology, 2011.

John, L., John, D. R., and John, P. S.: "Pressure Transient Testing," SPE Textbook Series, vol. 9, pp. 223-244, 2003

Jones, L.G. and Watts, J.W.: "Estimating skin effect in a partially completed damaged well" JPT (February 1971) 249-252

Kazemi, H.: "Effect of anisotropy and stratification on pressure transient analysis of wells with restricted flow entry". Journal of Canadian Petroleum Technology, May, 1969.

Khalmanova, K.: "A Mathematical Model of The Productivity Index of A Well". PhD Dissertation, Department of Mathematics, Texas A & M University, 2004.

Lu, J.: "New productivity formulae of partially penetrating wells". Journal of Canadian Petroleum Technology.

McDowell, J.M. and Muskat, M.: "The Effect on Well Productivity of Formation Penetration Beyond Perforated Casing," Trans. AIME (1950) 189, 309-312.

Muskat, M.: 'The Effect of Casing Perforations on Well Productivity," Trans. AIME (1943) lSl, 175-187.

Muskat, M.: "The Flow of Homogeneous Fluids through Porous Media". McGraw-Hill Book Co., Inc., New York City, USA, 1949.

Nisle, R. G.: "The effect of Partial Penetration on Pressure Build-Up in oil wells". Trans. AIME, Vol. 213, 1958.

Odeh, A.S.: "Steady-State Flow capacity of Wells with Limited Entry to Flow," Soc. Pet. Eng. J. (March 1968); Trans., AIME, 243.

Peacemean, D.W.: "Recalculation of Dietz Shape Factor for Rectangles". Unsolicited Paper, SPE 21256, 1990.

Reynolds, A.C., Chen, J. C., and Raghavan, R. : "Pseudo-skin factors caused by Partial Penetration," paper SPE 12178 presented at the 1983 SPE Annual Technical Conference and Exhibition, San Francisco, Oct, 5-8.

Saidikowski, R.M.: "Numerical simulation of the combined effects of wellbore damage and partial penetration" paper SPE 8204 presented at the 1979 SPE Annual Technical Conference, Las Vegas; September 23-26

Seth, M.S.: "Unsteady-State pressure distribution in a finite reservoir with partial wellbore opening". Journal of Canadian Petroleum Technology, December, 1968.

Stehfest, H.: "Numerical Inversion of Laplace Transforms," Algorithm 368, Communications of the ACM, Vol. 13, No.1 (January 1970) 47-49.

Streltsova-Adams, T.: "Pressure Drawdown in a Well with Limited Entry," J. Pel Tech. (Nov. 1979) 1469-1476.

Tiab, D., Katherine, M. Freddy, H. E., Matilde, M., Abel, C., Renzon, Z., Sandra, L. N.: "Determination of vertical and horizontal permeabilities for vertical oil and gas wells with partial completion and partial penetration using pressure and pressure derivative plots without type-curve matching", 2005

Yildiz, T.: "Assessment of total skin factor in perforated wells". SPE 82249, Colorado School of Mines. (2003).

APPENDIX A1: Closed System Pressure Derivation

From the partial form of the diffusivity equation,

$$\frac{\partial^2 P_D}{\partial r^2_D} + \frac{1}{r_D} \cdot \frac{\partial P_D}{\partial r_D} + \alpha \frac{\partial^2 P_D}{\partial z^2_D} = \frac{\partial P_D}{\partial t_D} \qquad (A1.1)$$

Inner boundary condition

$$C_D \frac{\partial P_{wD}}{d_{tD}} - \left(r_D \frac{\partial P_D}{\partial r_D} \right)_{r_D=1 \quad z_{D1} \leq z_D \leq z_{D2}} = 1 \qquad (A1.2)$$

$$P_{wD} = P_D - S \left(r_D \frac{\partial P_D}{\partial r_D} \right)_{r_D=1} \qquad (A1.3)$$

Outer Boundary condition

$$\left(\frac{\partial P_D}{\partial r_D} \right)_{r=reD} = 0 \qquad (A1.4)$$

Taking Laplace Transform of equation (A1.1); [u=Laplace variable]

$$\frac{d^2 \bar{P}_D}{dr_D^2} + \frac{1}{r_D} \cdot \frac{d\bar{P}_D}{dr_D} + \alpha \frac{d^2 \bar{P}_D}{dz_D^2} = u\bar{P}_D \qquad (A1.5)$$

Inner Boundary conditions

$$C_D u \bar{P}_D - \left(\frac{r_D d\bar{P}_D}{dr_D} \right)_{r_D=1} = \frac{1}{u} \qquad (A1.6)$$

$$\bar{P}_{wD} = \bar{P}_D - S \left(r_D \frac{\partial \bar{P}_D}{\partial r_D} \right)_{r_D=1} \qquad (A1.7)$$

Outer Boundary Condition

$$\left(\frac{\partial \bar{P}_D}{\partial r_D} \right)_{r=r_{eD}} = 0 \qquad (A1.8)$$

Taking Fourier Transform of equation (A1.5)

$$\frac{d^2 \widehat{\bar{P}_D}}{dr_D^2} + \frac{1}{r_D} \frac{d\widehat{\bar{P}}_D}{dr_D} - (n^2\pi^2\alpha + u)\widehat{\bar{P}}_D = 0 \qquad (A1.9)$$

Inner Boundary conditions

$$C_D u \bar{P}_{wD} - \left(\frac{r_D d\widehat{\bar{P}}_D}{dr_D} \right)_{r_D=1} = \frac{1}{u} \int_{z_{D1}}^{z_{D2}} \cos(n\pi z_D) dz_D \qquad (A1.10)$$

$$C_D u \widehat{\bar{P}}_{wD} - \left(\frac{r_D \partial \widehat{\bar{P}}_D}{dr_D} \right)_{r_D=1} = \frac{1}{n\pi u} [\sin(n\pi z_{D2}) - \sin(n\pi z_{D1})] \qquad (A1.11)$$

$$\hat{\bar{P}}_{wD} = \hat{\bar{P}}_D - S\left(r_D \frac{\partial \bar{P}_D}{\partial r_D}\right)_{r_D=1} \tag{A1.12}$$

Outer Boundary Condition

$$\left(\frac{\partial \hat{\bar{P}}_D}{\partial r_D}\right)_{r=r_{eD}} = 0 \tag{A1.13}$$

Equation (A1.9) is in Bessel form;

$$\hat{\bar{P}}_D = AI_0\left(r_D\sqrt{(n^2\pi^2\alpha + u)}\right) + BK_0\left(r_D\sqrt{(n^2\pi^2\alpha + u)}\right) \tag{A1.14}$$

From Outer B.C. Differentiating equation (A1.10) with respect to r_D

$$\left(\frac{d\hat{\bar{P}}_D}{dr_D}\right)_{r_D=1} = A\sqrt{(n^2\pi^2\alpha + u)}\, I_1\left(r_D\sqrt{n^2\pi^2\alpha + u}\right)$$

$$- B\sqrt{n^2\pi^2\alpha + u}\, K_1\left(r_D\sqrt{(n^2\pi^2\alpha + u)}\right) \tag{A1.15}$$

Let $n^2\pi^2\alpha + u = f$ and $r = r_{eD}$, $\left(\frac{\partial \bar{P}_D}{\partial r_D}\right)_{r=r_{eD}} = 0$

$$A\sqrt{f}I_1(r_{eD}\sqrt{f}) - B\sqrt{f}K_1(r_{eD}\sqrt{f}) = 0 \tag{A1.16}$$

$$A = \frac{B\sqrt{f}K_1(r_{eD}\sqrt{f})}{\sqrt{f}I_1(r_{eD}\sqrt{f})} = \frac{BK_1(r_{eD}\sqrt{f})}{I_1(r_{eD}\sqrt{f})} \tag{A1.17}$$

Therefore, $\left(\frac{\partial \hat{\bar{P}}_D}{\partial r_D}\right)_{r_D=1} = A\sqrt{f}I_1(\sqrt{f}) - B\sqrt{f}K_1(\sqrt{f})$ $\tag{A1.18}$

Substitute equation (A1.18) and (A1.9) into equation (A1.16)

$$\hat{\bar{P}}_{wD} = AI_0(\sqrt{f}) + BK_0(\sqrt{f}) - S[A\sqrt{f}I_1(\sqrt{f}) - B\sqrt{f}K_1(\sqrt{f})] \tag{A1.19}$$

Substitute for A in equation (A1.19) with equation (A1.17)

$$\hat{\bar{P}}_{wD} = \frac{BK_1(r_{eD}\sqrt{f})}{I_1(r_{eD}\sqrt{f})}I_0(\sqrt{f}) + BK_0\sqrt{f}$$

$$- S\left[\frac{BK_1(\sqrt{f})(r_{eD}\sqrt{f})}{I_1(r_{eD}\sqrt{f})} \cdot I_1(\sqrt{f}) - B\sqrt{f}K_1(\sqrt{f})\right] \tag{A1.20}$$

Multiply through by $I_1(r_{eD}\sqrt{f})$

$\hat{\bar{P}}_{wD}$

$$= \frac{BK_1(r_{eD}\sqrt{f})I_0\sqrt{f} + BK_0\sqrt{f}I_1(r_{eD}\sqrt{f}) - SBK_1(\sqrt{f})(r_{eD}\sqrt{f})I_1(\sqrt{f}) + SB\sqrt{f}K_1(\sqrt{f})I_1(r_{eD}\sqrt{f})}{I_1(r_{eD}\sqrt{f})}$$

$$\tag{A1.21}$$

$\hat{\bar{P}}_{wD}I_1(r_{eD}\sqrt{f}) = B[K_1(r_{eD}\sqrt{f})I_0\sqrt{f} + K_0\sqrt{f}I_1(r_{eD}\sqrt{f}) - SK_1(\sqrt{f})(r_{eD}\sqrt{f})I_1(\sqrt{f}) +$

$S\sqrt{f}K_1(\sqrt{f})I_1(r_{eD}\sqrt{f})]$ $\tag{A1.22}$

$$B = \frac{\hat{\bar{P}}_{wD} I_1\left(r_{eD}\sqrt{f}\right)}{\left[K_1\left(r_{eD}\sqrt{f}\right)I_0\sqrt{f} + K_0\sqrt{f}I_1\left(r_{eD}\sqrt{f}\right) - SK_1\left(\sqrt{f}\right)\left(r_{eD}\sqrt{f}\right)I_1\left(\sqrt{f}\right) + S\sqrt{f}K_1\left(\sqrt{f}\right)I_1\left(r_{eD}\sqrt{f}\right)\right]}$$

$$(A1.23)$$

$$A = \frac{\hat{\bar{P}}_{wD} K_1\left(r_{eD}\sqrt{f}\right)}{\left[K_1\left(r_{eD}\sqrt{f}\right)I_0\sqrt{f} + K_0\sqrt{f}I_1\left(r_{eD}\sqrt{f}\right) - SK_1\left(\sqrt{f}\right)\left(r_{eD}\sqrt{f}\right)I_1\left(\sqrt{f}\right) + S\sqrt{f}K_1\left(\sqrt{f}\right)I_1\left(r_{eD}\sqrt{f}\right)\right]}$$

$$(A1.24)$$

$$\left(\frac{d\hat{\bar{P}}_D}{dr_D}\right)_{r_{D=1}}$$

$$= \frac{\hat{\bar{P}}_{wD}\sqrt{f}K_1\left(r_{eD}\sqrt{f}\right)I_1\sqrt{f} - \hat{\bar{P}}_{wD}\sqrt{f}I_1\left(r_{eD}\sqrt{f}\right)K_1\sqrt{f}}{\left[K_1\left(r_{eD}\sqrt{f}\right)I_0\sqrt{f} + K_0\sqrt{f}I_1\left(r_{eD}\sqrt{f}\right) - SK_1\left(\sqrt{f}\right)\left(r_{eD}\sqrt{f}\right)I_1\left(\sqrt{f}\right) + S\sqrt{f}K_1\left(\sqrt{f}\right)I_1\left(r_{eD}\sqrt{f}\right)\right]}$$

$$(A1.25)$$

From the inner boundary condition of the wellbore storage (A1.11), substitute equation (A1.25);

$$C_D u \hat{\bar{P}}_{wD}$$

$$- \frac{\hat{\bar{P}}_{wD}\sqrt{f}K_1\left(r_{eD}\sqrt{f}\right)I_1\sqrt{f} - \hat{\bar{P}}_{wD}\sqrt{f}I_1\left(r_{eD}\sqrt{f}\right)K_1\sqrt{f}}{\left[K_1\left(r_{eD}\sqrt{f}\right)I_0\sqrt{f} + K_0\sqrt{f}I_1\left(r_{eD}\sqrt{f}\right) - SK_1\left(\sqrt{f}\right)\left(r_{eD}\sqrt{f}\right)I_1\left(\sqrt{f}\right) + S\sqrt{f}K_1\left(\sqrt{f}\right)I_1\left(r_{eD}\sqrt{f}\right)\right]}$$

$$= \frac{1}{n\pi u}\left[\sin(n\pi z_{D2}) - \sin(n\pi z_{D1})\right] \qquad (A1.26)$$

Now let:

$$\theta = \frac{1}{n\pi u}\left[\sin(n\pi z_{D2}) - \sin(n\pi z_{D1})\right]\left[K_1\left(r_{eD}\sqrt{f}\right)I_0\sqrt{f} + K_0\sqrt{f}I_1\left(r_{eD}\sqrt{f}\right)\right.$$

$$\left. - SK_1\left(\sqrt{f}\right)\left(r_{eD}\sqrt{f}\right)I_1\left(\sqrt{f}\right) + S\sqrt{f}K_1\left(\sqrt{f}\right)I_1\left(r_{eD}\sqrt{f}\right)\right] \qquad (A1.27a)$$

$$\exists = \left[C_D u\left[K_1\left(r_{eD}\sqrt{f}\right)I_0\sqrt{f} + K_0\sqrt{f}I_1\left(r_{eD}\sqrt{f}\right) - SK_1\left(\sqrt{f}\right)\left(r_{eD}\sqrt{f}\right)I_1\left(\sqrt{f}\right)\right.\right.$$

$$\left.\left. + S\sqrt{f}K_1\left(\sqrt{f}\right)I_1\left(r_{eD}\sqrt{f}\right)\right]\right] - \sqrt{f}K_1\left(r_{eD}\sqrt{f}\right)I_1\sqrt{f} + \sqrt{f}I_1\left(r_{eD}\sqrt{f}\right)K_1\sqrt{f}$$

$$(A1.27b)$$

$$\hat{\bar{P}}_{wD} = \frac{\theta}{\exists} \qquad (A1.27c)$$

Invert from Fourier to Laplace space

$$\hat{\bar{P}}_{wD} = \frac{1}{h_{fD}}\sum_{n=0}^{\infty}\frac{\theta}{\exists}\left(\cos n\pi z_D\right) \qquad (A1.28)$$

$$\lim as\ n \to 0$$

$$\lim_{n\to 0}\frac{\theta}{\exists}\left(\cos n\pi z_D\right) \qquad (A1.29)$$

Taking limits: $n \to 0$, sin(n)=n, cos(n)=1, tan(n)=0, note $\sqrt{f} = \sqrt{n^2\pi^2\alpha + u} = \sqrt{u}$ as $n \to 0$

$$G = \left[K_1\left(r_{eD}\sqrt{u}\right)I_0\sqrt{u} + K_0\sqrt{f}I_1\left(r_{eD}\sqrt{u}\right) - SK_1\left(\sqrt{u}\right)\left(r_{eD}\sqrt{u}\right)I_1\left(\sqrt{u}\right)\right.$$
$$\left. + S\sqrt{f}K_1\left(\sqrt{u}\right)I_1\left(r_{eD}\sqrt{u}\right)\right] \qquad (A1.30a)$$

Now, from equation (A1.30a) and (A1.27b);

$$\bar{P}_{wD} = \frac{(z_{D2} - z_{D1})G}{\exists} \qquad (A1.30b)$$

Now, $h_{fD} = z_{D2} - z_{D1}$

$$\bar{P}_{wD} = \frac{1}{h_{fD}}\left[\frac{(z_{D2} - z_{D1})G}{\exists}\right.$$
$$\left. + \left[\frac{1}{h_{fD}}\sum_{n=1}^{\infty}\frac{1}{n\pi u}\left(\frac{[\sin(n\pi z_{D2}) - \sin(n\pi z_{D1})]G}{\exists}\right)(\cos n\pi z_D)\right]\right] \qquad (A1.31)$$

$$\bar{P}_{wD} = \frac{G}{\exists} + \left[\frac{1}{h_{fD}}\sum_{n=1}^{\infty}\frac{1}{n\pi u}\left(\frac{[\sin(n\pi z_{D2}) - \sin(n\pi z_{D1})]G}{\exists}\right)(\cos n\pi z_D)\right] \qquad (A1.32)$$

Final Equations for Closed system after inversion from Laplace space

$$P_{wD} = \frac{5.274 \times 10^{-4}kt}{\emptyset\mu C_t r_e^2} - \frac{3}{4} + ln\left(\frac{r_e}{r_w}\right)$$
$$+ \frac{1}{hfD}\sum_{n=1}^{\infty}\frac{-1}{n^2\pi^2\sqrt{\alpha}}\left\{\left[\frac{K_1\left(r_{eD}n\pi\sqrt{\alpha}\right)I_0\left(n\pi\sqrt{\alpha}\right) + K_0\left(n\pi\sqrt{\alpha}\right)I_1\left(r_{eD}n\pi\sqrt{\alpha}\right)}{K_1\left(r_{eD}n\pi\sqrt{\alpha}\right)I_1\left(n\pi\sqrt{\alpha}\right) - I_1\left(r_{eD}n\pi\sqrt{\alpha}\right)K_1\left(n\pi\sqrt{\alpha}\right)}\right]\right.$$
$$\left. \cdot [\cos(n\pi z_D)((\sin(n\pi z_{D2}) - \sin(n\pi z_{D1}))]\right\} \qquad (A1.33)$$

- C_D is the dimensionless wellbore storage and S is the skin
- u is the Laplace space variable, K_0 and K_1 are the modified Bessel K, second kind of order zero and one respectively
- I_0 and I_1 are modified Bessel I, first kind of the order zero and one respectively.
- h_{fD} is the dimensionless thickness of the ratio $\frac{h_p}{h}$

APPENDIX A2: Constant Pressure Boundary Pressure Derivation

From the partial form of the diffusivity equation,

$$\frac{\partial^2 P_D}{\partial r^2_D} + \frac{1}{r_D} \cdot \frac{\partial P_D}{\partial r_D} + \alpha \frac{\partial^2 P_D}{\partial z^2_D} = \frac{\partial P_D}{\partial t_D} \qquad (A2.1)$$

Inner boundary conditions

$$C_D \frac{\partial P_{wD}}{d_{tD}} - \left(r_D \frac{\partial P_D}{\partial r_D}\right)_{r_{D=1}} \bigg|_{z_{D1} \leq z_D \leq z_{D2}} = 1 \qquad (A2.2)$$

$$P_{wD} = P_D - S\left(r_D \frac{\partial P_D}{\partial r_D}\right)_{r_{D=1}} \qquad (A2.3)$$

Outer Boundary condition;

$$P_D(r_{eD}, t_D) = 0 \qquad\qquad r_{eD} = \frac{r_e}{r_w} \qquad (A2.4)$$

Taking Laplace Transform; [u=Laplace variable]

$$\frac{d^2 \bar{P}_D}{dr_D^2} + \frac{1}{r_D} \cdot \frac{d\bar{P}_D}{dr_D} + \alpha \frac{d^2 \bar{P}_D}{dz_D^2} = u\bar{P}_D \qquad (A2.5)$$

Inner Boundary conditions

$$C_D u \bar{P}_D - \left(\frac{r_D d\bar{P}_D}{dr_D}\right)_{r_{D=1}} = \frac{1}{u} \qquad (A2.6)$$

$$\bar{P}_{wD} = \bar{P}_D - S\left(r_D \frac{\partial \bar{P}_D}{\partial r_D}\right)_{r_{D=1}} \qquad (A2.7)$$

Taking Fourier Transform

$$\frac{d^2 \widehat{\bar{P}_D}}{dr_D^2} + \frac{1}{r_D} \frac{d\widehat{\bar{P}}_D}{dr_D} - (n^2 \pi^2 \alpha + u)\widehat{\bar{P}}_D = 0 \qquad (A2.8)$$

Inner Boundary Conditions

$$C_D u \bar{P}_{wD} - \left(\frac{r_D d\widehat{\bar{P}}_D}{dr_D}\right)_{r_{D=1}} = \frac{1}{u} \int_{Z_{D1}}^{Z_{D2}} \cos(n\pi z_D) dz_D \qquad (A2.9)$$

$$C_D u \hat{\bar{P}}_{wD} - \left(\frac{r_D \partial \hat{\bar{P}}_D}{dr_D} \right)_{r_{D=1}} = \frac{1}{n\pi u} [\sin(n\pi z_{D2}) - \sin(n\pi z_{D1})] \tag{A2.10}$$

$$\hat{\bar{P}}_{wD} = \hat{\bar{P}}_D - S \left(r_D \frac{\partial \bar{P}_D}{\partial r_D} \right)_{r_{D=1}} \tag{A2.11}$$

Outer B.C

$$\hat{\bar{P}}_D(r_{eD}, u) = 0 \qquad r_{eD} = \frac{r_e}{r_w} \tag{A2.12}$$

Now, from equation (A2.8), Solution is in Bessel function form as

$$\hat{\bar{P}}_D = A I_0 \left(r_D \sqrt{(n^2\pi^2\alpha + u)} \right) + B K_0 \left(r_D \sqrt{(n^2\pi^2\alpha + u)} \right) \tag{A2.13}$$

Differentiating with respect to r_D

$$\left(\frac{d\hat{\bar{P}}_D}{dr_D} \right)_{r_{D=1}} = A\sqrt{(n^2\pi^2\alpha + u)} \, I_1 \left(r_D \sqrt{n^2\pi^2\alpha + u} \right)$$

$$- B\sqrt{n^2\pi^2\alpha + u} \, K_1 \sqrt{n^2\pi^2\alpha + u} \tag{A2.14}$$

Let $n^2\pi^2\alpha + u = f \; and \; r_D = r_{eD}$,

From outer Boundary Condition;

$$P_D(r_{eD}, u) = 0 \tag{A2.15}$$

Therefore

$$A I_0(r_D\sqrt{f}) + B K_0(r_D\sqrt{f}) = 0 \tag{A2.16}$$

$$A = -\frac{B K_0(r_{eD}\sqrt{f})}{I_0(r_{eD}\sqrt{f})} \tag{A2.17}$$

Therefore;

$$\left(\frac{d\hat{\bar{P}}_D}{dr_D} \right)_{r_{D=1}} = A\sqrt{f} I_1(r_{eD}\sqrt{f}) - B\sqrt{f} K_1(r_{eD}\sqrt{f}) = 0 \tag{A2.18}$$

Substitute equation (A2.13) and (A2.14) into equation (A2.11)

$$\hat{\bar{P}}_{wD} = A I_0(\sqrt{f}) + B K_0(\sqrt{f}) - S[A\sqrt{f} I_1(\sqrt{f}) - B\sqrt{f} K_1(\sqrt{f})] \tag{A2.19}$$

Substituting equation (A2.17) into equation (A2.19), we obtain:

$$\hat{\bar{P}}_{wD} = \frac{-B K_0(r_{eD}\sqrt{f})}{I_0(r_{eD}\sqrt{f})} \cdot I_0(\sqrt{f}) + B K_0\sqrt{f}$$

$$- S \left[\frac{B K_0(\sqrt{f})(r_{eD}\sqrt{f})}{I_0(r_{eD}\sqrt{f})} \cdot I_1(\sqrt{f}) - B\sqrt{f} K_1(\sqrt{f}) \right] \tag{A2.20}$$

Multiplying through by $I_0(r_{eD}\sqrt{f})$;

$$\bar{\bar{P}}_{wD}$$

$$= \frac{-BK_0(r_{eD}\sqrt{f})I_0\sqrt{f} + BK_0\sqrt{f}I_0(r_{eD}\sqrt{f}) + SB(\sqrt{f})K_0(r_{eD}\sqrt{f})I_1(\sqrt{f}) + SB\sqrt{f}K_1(\sqrt{f})I_0(r_{eD}\sqrt{f})}{I_0(r_{eD}\sqrt{f})}$$

$$(A2.21)$$

$$B$$

$$= \frac{\bar{\bar{P}}_{wD}I_0(r_{eD}\sqrt{f})}{\left[-K_0(r_{eD}\sqrt{f})I_0\sqrt{f} + K_0\sqrt{f}I_0(r_{eD}\sqrt{f}) + S(\sqrt{f})K_0(r_{eD}\sqrt{f})I_1(\sqrt{f}) + S\sqrt{f}K_1(\sqrt{f})I_0(r_{eD}\sqrt{f})\right]}$$

$$(A2.22)$$

Substitute (A2.22) into equation (A2.16)

$$A$$

$$= \frac{\bar{\bar{P}}_{wD}K_0(r_{eD}\sqrt{f})}{\left[-K_0(r_{eD}\sqrt{f})I_0\sqrt{f} + K_0\sqrt{f}I_0(r_{eD}\sqrt{f}) + SK_0(\sqrt{f})(r_{eD}\sqrt{f})I_1(\sqrt{f}) + S\sqrt{f}K_1(\sqrt{f})I_0(r_{eD}\sqrt{f})\right]}$$

$$(A2.23)$$

Substitute (A2.22) and (A2.23) into equation (A2.18)

$$\left(\frac{d\bar{\bar{P}}_D}{dr_D}\right)_{r_{D=1}}$$

$$= \frac{\bar{\bar{P}}_{wD}\sqrt{f}K_0(r_{eD}\sqrt{f})I_1(\sqrt{f}) - \bar{\bar{P}}_{wD}\sqrt{f}I_0(r_{eD}\sqrt{f})K_1(\sqrt{f})}{\left[-K_0(r_{eD}\sqrt{f})I_0\sqrt{f} + K_0\sqrt{f}I_0(r_{eD}\sqrt{f}) + SK_0(\sqrt{f})(r_{eD}\sqrt{f})I_1(\sqrt{f}) + S\sqrt{f}K_1(\sqrt{f})I_0(r_{eD}\sqrt{f})\right]}$$

$$(A2.24)$$

From well bore storage equation, (A2.10), substitute equation (A2.24) into that inner boundary condition

$$C_D u\bar{\bar{P}}_{wD}$$

$$- \frac{-\bar{\bar{P}}_{wD}\sqrt{f}K_0(r_{eD}\sqrt{f})I_1(\sqrt{f}) + \bar{\bar{P}}_{wD}\sqrt{f}I_0(r_{eD}\sqrt{f})K_1(\sqrt{f})}{\left[-K_0(r_{eD}\sqrt{f})I_0\sqrt{f} + K_0\sqrt{f}I_0(r_{eD}\sqrt{f}) + SK_0(\sqrt{f})(r_{eD}\sqrt{f})I_1(\sqrt{f}) + S\sqrt{f}K_1(\sqrt{f})I_0(r_{eD}\sqrt{f})\right]}$$

$$= \frac{1}{n\pi u}[\sin(n\pi z_{D2}) - \sin(n\pi z_{D1})] \qquad (A2.25)$$

Multiply through by the denominator and make $\bar{\bar{P}}_{wD}$ the subject

Let the denominator be represented by the letter X

$$C_D u\bar{\bar{P}}_{wD}.X - \left(-\bar{\bar{P}}_{wD}\sqrt{f}K_0(r_{eD}\sqrt{f})I_1(\sqrt{f}) + \bar{\bar{P}}_{wD}\sqrt{f}I_0(r_{eD}\sqrt{f})K_1(\sqrt{f})\right)$$

$$= \frac{X}{n\pi u}[\sin(n\pi z_{D2}) - \sin(n\pi z_{D1})] \qquad (A2.26)$$

Let D and E represent the following;

$$D = [\sin(n\pi z_{D2}) - \sin(n\pi z_{D1})][-K_0(r_{eD}\sqrt{f})I_0\sqrt{f} + K_0\sqrt{f}I_0(r_{eD}\sqrt{f})$$
$$+ SK_0(\sqrt{f})(r_{eD}\sqrt{f})I_1(\sqrt{f}) + S\sqrt{f}K_1(\sqrt{f})I_0(r_{eD}\sqrt{f})]$$

And

$$E =$$

$$\left(C_D u[-K_0(r_{eD}\sqrt{f})I_0\sqrt{f} + K_0\sqrt{f}I_0(r_{eD}\sqrt{f}) + SK_0(\sqrt{f})(r_{eD}\sqrt{f})I_1(\sqrt{f}) +\right.$$

$$S\sqrt{f}K_1(\sqrt{f})I_0(r_{eD}\sqrt{f})] + \sqrt{f}K_0(r_{eD}\sqrt{f})I_1(\sqrt{f}) -$$

$$\left.\sqrt{f}I_0(r_{eD}\sqrt{f})K_1(\sqrt{f})\right)$$

Therefore, we can write the dimensionless pressure at the wellbore as:

$$\hat{\bar{P}}_{wD} = \frac{1}{n\pi u}\frac{D}{E} \tag{A2.27}$$

<div align="center">Inversion from Fourier to Laplace space</div>

$$\bar{P}_{wD} = \frac{1}{h_{fD}}\sum_{n=1}^{\infty}\frac{1}{n\pi u}\frac{D}{E} \tag{A2.28}$$

<div align="center">$\lim as\ n \to 0$</div>

$$\lim_{n\to 0}\frac{1}{n\pi u}\frac{D}{E} \tag{A2.29}$$

Taking limits: $n \to 0$, sin(n)=n, cos(n)=1, tan(n)=0, note $\sqrt{f} = \sqrt{n^2\pi^2\alpha + u} = \sqrt{u}$ $as\ n \to 0$

Let

$$F = [-K_0(r_{eD}\sqrt{f})I_0\sqrt{f} + K_0\sqrt{f}I_0(r_{eD}\sqrt{f}) + SK_0(\sqrt{f})(r_{eD}\sqrt{f})I_1(\sqrt{f}) + S\sqrt{f}K_1(\sqrt{f})I_0(r_{eD}\sqrt{f})]$$

$$\bar{P}_{wD} = \frac{(z_{D2} - z_{D1})*F}{E} \tag{A2.30}$$

Now, $h_{fD} = z_{D2} - z_{D1}$

$$\bar{P}_{wD} = \frac{1}{h_{fD}}\frac{(z_{D2} - z_{D1})*F}{E} + \frac{1}{h_{fD}}\sum_{n=1}^{\infty}\frac{1}{n\pi u}\frac{D\cos(n\pi z_D)}{E} \tag{A2.31}$$

$$\bar{P}_{wD} = \frac{F}{E} + \frac{1}{h_{fD}}\sum_{n=1}^{\infty}\frac{1}{n\pi u}\frac{D\cos(n\pi z_D)}{E} \tag{A2.32}$$

$C_D \to 0$ and $S \to 0$, and leaves the above dimensionless pressure equation at the well without skin and wellbore storage effects as shown in the equation below:

$$\bar{P}_{wD}$$

$$= \frac{-1}{u^{\frac{3}{2}}}\left[\frac{K_0(r_{eD}\sqrt{u})I_0(\sqrt{u}) - K_0(\sqrt{u})I_0(r_{eD}\sqrt{u})}{K_0(r_{eD}\sqrt{u})I_1(\sqrt{u}) + I_0(r_{eD}\sqrt{u})K_1(\sqrt{u})}\right]$$

$$+ \frac{1}{hfD}\sum_{n=1}^{\infty}\frac{-1}{n\pi u}\left[\frac{(\sin n\pi z_{D2} - \sin n\pi z_{D1})K_0(r_{eD}\sqrt{f})I_0(\sqrt{f}) - K_0(\sqrt{f})I_0(r_{eD}\sqrt{f})}{\sqrt{f}K_1(r_{eD}\sqrt{f})I_1(\sqrt{f}) + \sqrt{f}I_1(r_{eD}\sqrt{f})K_1(\sqrt{f})}\right]$$

$$\times \cos(n\pi z_D) \qquad\qquad (A2.33)$$

This is the equation after inverting from Laplace space

$$P_{wD} = ln(r_{eD})$$

$$+ \frac{1}{hfD}\sum_{n=1}^{\infty}\frac{-1}{n^2\pi^2\sqrt{\alpha}}\left\{\left[\frac{K_0(r_{eD}n\pi\sqrt{\alpha})I_0(n\pi\sqrt{\alpha}) - K_0(n\pi\sqrt{\alpha})I_1(r_{eD}n\pi\sqrt{\alpha})}{K_0(r_{eD}n\pi\sqrt{\alpha})I_1(n\pi\sqrt{\alpha}) + I_0(r_{eD}n\pi\sqrt{\alpha})K_1(n\pi\sqrt{\alpha})}\right]\right.$$

$$\left. * \cos(\cos n\pi z_D)\left[\sin(n\pi z_{D2}) - \sin(n\pi z_{D1})\right]\right\} \qquad\qquad (A2.34)$$

- C_D and S are the dimensionless wellbore storage and skin respectively

- u, K_0, K_1, I_0, I_1, h_{fD} have the same meaning as defined in Appendix A1.

PREAMBLE TO THE GENERAL SOLUTION TO APPENDIX B1, B2 and B3

The general expression for ΔP at an arbitrary point (x,y,z) was obtained by integrating the

appropriate point sink functions. The vertical well (line sink) is parallel to the z-axis and located

along x=x_o, y=y_o, and $z_1 \leq z \leq z_2$.

These point sink functions were integrated twice along the vertical direction (z) of the well and

time τ, in order to obtain a line source solution as seen in the following expressions:

$$\Delta P = P_i - P(x,y,z,t) = \left[\frac{886.9 B\mu q}{abhL\alpha}\right] \int_0^t \int_{z_1}^{z_2} (S_1.S_2.S_3)\, dz_o d\tau \qquad (B.1)$$

With:

$$\alpha = 157.952 \emptyset \mu C_t \ days \qquad (B.2)$$

$$L = (z_2 - z_1) \rightarrow lenght\ of\ vertical\ well, ft \qquad (B.3)$$

S_1, S_2, S_3 denote the point sink functions. Carslaw and Jaegar have shown that T is time.

And a, b and h are distances in the x, y and z directions, and for an anisotropy case, a, b and h are

not equal and also $k_x \neq k_y$; $x_o \neq y_o$; and $\sqrt{\frac{k_y}{k_x}} \neq 1$. $x_o, y_o,$ and $z_o = z$ are respectively the well

positions in the x direction, y direction and the z direction.

The reservoir is considered to be of a rectangular shape with the well at its centre.

APPENDIX B1: Closed System

The following point source functions depicting a no-flow boundary case from Gringarten and

Ramey are used. Here, S_1 , S_2, and S_3 are the instantaneous point sink functions (Green's Functions)

located at (x_o, y_o, z_o) and satisfying the zero flux boundary conditions at x = 0, a; y= 0, and z = 0.

$$S_1 = S_1(x,x_o,\tau) = 1 + 2\sum_{n=1}^{\infty} \cos\frac{n\pi x}{a} \cos\frac{n\pi x_o}{a} exp\left[-\frac{n^2\pi^2 k_x \tau}{\alpha a^2}\right] \qquad (B1.1)$$

$$S_2 = S_2(y,y_o,\tau) = 1 + 2\sum_{m=1}^{\infty} \cos\frac{m\pi y}{b} \cos\frac{m\pi y_o}{b} exp\left[-\frac{m^2\pi^2 k_y \tau}{\alpha b^2}\right] \qquad (B1.2)$$

$$S_3 = S_3(z,z_o,\tau) = 1 + 2\sum_{l=1}^{\infty} \cos\frac{l\pi z}{h} \cos\frac{l\pi z_o}{h} exp\left[-\frac{l^2\pi^2 k_z \tau}{\alpha h^2}\right] \qquad (B1.3)$$

These Green's functions can be expressed as:

$$\int_0^t \int_{z_1}^{z_2} (S_1.S_2.S_3)\, dz_o d\tau$$

$$= \left[\frac{886.9B\mu q}{abh\alpha}\right]\left[t + \frac{2\alpha a^2}{\pi^2 k_x}\sum_{n=1}^{\infty}\frac{\cos\frac{n\pi x}{a}\cos\frac{n\pi x_o}{a}}{n^2}\left(1 - exp\left(\frac{-n^2\pi^2 k_x t}{\alpha a^2}\right)\right)\right.$$

$$+ \frac{2\alpha a^2}{\pi^2 k_y}\sum_{m=1}^{\infty}\frac{\cos\frac{m\pi y}{a}\cos\frac{m\pi y_o}{a}}{m^2}\left(1 - exp\left(\frac{-m^2\pi^2 k_y t}{\alpha b^2}\right)\right)$$

$$+ \frac{4\alpha}{\pi^2}\sum_{n,m}^{\infty}\frac{\cos\frac{n\pi x}{a}\cos\frac{n\pi x_o}{a}\cos\frac{m\pi y}{b}\cos\frac{m\pi y_o}{b}}{\left[\frac{n^2 k_x}{a^2}+\frac{m^2 k_y}{b^2}\right]}\left(1 - exp\left(\frac{-n^2\pi^2 k_x t}{\alpha a^2}\frac{-m^2\pi^2 k_y t}{\alpha b^2}\right)\right)$$

$$+ \frac{2\alpha h^3}{\pi^3 k_z(z_2 - z_1)}\sum_{l}\frac{\cos\frac{l\pi z}{h}\left[\frac{\sin\frac{l\pi z_2}{h}}{h}-\frac{\sin\frac{l\pi z_1}{h}}{h}\right]}{l^3}\left(1 - exp\left(\frac{-l^2\pi^2 k_z t}{\alpha h^2}\right)\right)$$

$$+ \frac{4\alpha h}{\pi^3(z_2 - z_1)}\sum_{l,n}\frac{\cos\frac{n\pi x}{a}\cos\frac{n\pi x_o}{a}\cos\frac{l\pi z}{h}\left[\frac{\sin\frac{l\pi z_2}{h}}{h}-\frac{\sin\frac{l\pi z_1}{h}}{h}\right]}{l\left[\frac{n^2 k_x}{a^2}+\frac{l^2 k_z}{h^2}\right]}\left(1\right.$$

$$\left.- exp\left(\frac{-l^2\pi^2 k_z t}{\alpha h^2}\frac{-n^2\pi^2 k_X t}{\alpha a^2}\right)\right)a$$

$$+ \frac{4\alpha h}{\pi^3(z_2 - z_1)}\sum_{l,m}\frac{\cos\frac{m\pi y}{b}\cos\frac{m\pi y_o}{b}\cos\frac{l\pi z}{h}\left[\frac{\sin\frac{l\pi z_2}{h}}{h}-\frac{\sin\frac{l\pi z_1}{h}}{h}\right]}{l\left[\frac{m^2 k_y}{b^2}+\frac{l^2 k_z}{h^2}\right]}\left(1\right.$$

$$\left.- exp\left(\frac{-l^2\pi^2 k_z t}{\alpha h^2}\frac{-m^2\pi^2 k_y t}{\alpha b^2}\right)\right)$$

$$+ \frac{4\alpha h}{\pi^2(z_2 - z_1)}\sum_{n,l,m}^{\infty}\frac{\cos\frac{n\pi x}{a}\cos\frac{n\pi x_o}{a}\cos\frac{m\pi y}{b}\cos\frac{m\pi y_o}{b}\cos\frac{l\pi z}{h}\left[\frac{\sin\frac{l\pi z_2}{h}}{h}-\frac{\sin\frac{l\pi z_1}{h}}{h}\right]}{l\left[\frac{n^2 k_x}{a^2}+\frac{m^2 k_y}{b^2}+\frac{l^2 k_z}{h^2}\right]}\left(1\right.$$

$$\left.\left.- exp\left(\frac{-l^2\pi^2 k_z t}{\alpha h^2}\frac{-n^2\pi^2 k_x t}{\alpha a^2}\frac{-m^2\pi^2 y t}{\alpha b}\right)\right)\right] \tag{B1.4}$$

For pseudo steady state (large time) behaviour of ΔP in the equation above, let $t \to \infty$, and the all terms in the exponential factors are dropped:

$$P_i - P(x, y, z; t \to \infty) =$$

$$\left[\frac{886.9B\mu q}{\alpha abh}\right]\left[t\frac{ab}{2\pi\sqrt{k_x k_y}}\left(P_x + P_y + P_z + P_{xy} + P_{xz} + P_{yz} + P_{xyz}\right)\right] \tag{B1.5}$$

Where:

$$P_x = \frac{4a}{\pi b}\sqrt{\frac{k_y}{k_x}}\sum_{n=1} \frac{\cos\frac{n\pi x}{a}\cos\frac{n\pi x_o}{a}}{n^2} \tag{B1.6}$$

$$P_y = \frac{4b}{\pi a}\sqrt{\frac{k_x}{k_y}}\sum_{m=1} \frac{\cos\frac{m\pi y}{b}\cos\frac{m\pi y_o}{b}}{m^2} \tag{B1.7}$$

$$P_z = \left[\frac{4h^3\sqrt{k_xk_y}}{\pi^2 Labk_z}\right]\sum_{l=1} \frac{\cos\frac{l\pi z}{h}\left[\frac{\sin\frac{l\pi z_2}{h}-\frac{\sin\frac{l\pi z_1}{h}}{}\right]}{l^3} \tag{B1.8}$$

$$P_{xy} = \left[\frac{8\sqrt{k_xk_y}}{\pi ab}\right]\sum_{n,m=1} \frac{\cos\frac{n\pi x}{a}\cos\frac{n\pi x_o}{a}\cos\frac{m\pi y}{b}\cos\frac{m\pi y_o}{b}}{\left[\frac{n^2k_x}{a^2}+\frac{m^2k_y}{b^2}\right]} \tag{B1.9}$$

$$P_{xz} = \left[\frac{8h\sqrt{k_xk_y}}{\pi^2 Lab}\right]\sum_{n,l=1} \frac{\cos\frac{n\pi x}{a}\cos\frac{n\pi x_o}{a}\cos\frac{l\pi z}{h}\left[\frac{\sin\frac{l\pi z_2}{h}-\frac{\sin\frac{l\pi z_1}{h}}{}\right]}{l\left[\frac{n^2k_x}{a^2}+\frac{l^2k_z}{h^2}\right]} \tag{B1.10}$$

$$P_{yz} = \left[\frac{8h\sqrt{k_xk_y}}{\pi^2 Lab}\right]\sum_{n,l=1} \frac{\cos\frac{n\pi x}{b}\cos\frac{n\pi x_o}{b}\cos\frac{l\pi z}{h}\left[\frac{\sin\frac{l\pi z_2}{h}-\frac{\sin\frac{l\pi z_1}{h}}{}\right]}{l\left[\frac{m^2k_y}{b^2}+\frac{l^2k_z}{h^2}\right]} \tag{B1.11}$$

P_{xyz}

$$= \left[\frac{16h\sqrt{k_xk_y}}{\pi^2 Lab}\right]\sum_{n,l,m=1} \frac{\cos\frac{n\pi x}{a}\cos\frac{n\pi x_o}{a}\cos\frac{m\pi y}{b}\cos\frac{m\pi y_o}{b}\cos\frac{l\pi z}{h}\left[\frac{\sin\frac{l\pi z_2}{h}-\frac{\sin\frac{l\pi z_1}{h}}{}\right]}{l\left[\frac{n^2k_x}{a^2}+\frac{m^2k_y}{b^2}+\frac{l^2k_z}{h^2}\right]} \tag{B1.12}$$

By averaging equation three over the entire reservoir region $0 \le x \le a, 0 \le y \le b, 0 \le z \le h$, we obtain [$(Px + Py + Pz + Pxy + Pzx + Pzy + Pxyz)$average to zero identically]

Therefore equation (B1.5) becomes:

$$P_i - \bar{P}_R = \left[\frac{886.9B\mu q}{\alpha a^2 h}\right]t \tag{B1.13}$$

Now subtracting equation (B1.13) from equation (B1.15), yields the general formula for the pseudo steady state pressure drop at an arbitrary point (x,y,z) in the reservoir.

$$\Delta P = (\bar{P}_R - P) = \left[\frac{141.15B\mu q}{h\sqrt{k_xk_y}}\right][P_x + P_y + P_z + P_{xy} + P_{xz} + P_{yz} + P_{xyz}] \tag{B1.14}$$

The above equation is for partial penetration

For full completion:

$$\Delta P = (\bar{P}_R - P) = \left[\frac{141.15B\mu q}{h\sqrt{k_xk_y}}\right][P_x + P_y + P_{xy}] \tag{B1.16}$$

64

APPENDIX B2: Bottom Water

The flowing point source functions from Gringarten and Ramey are used.

Recall S_1 and S_2 from Appendix B1;

$$S_1 = S_1(x, x_o, \tau) = 1 + 2 \sum_{n=1}^{\infty} \cos\frac{n\pi x}{a} \cos\frac{n\pi x_o}{a} \, exp\left[-\frac{n^2\pi^2 k_x \tau}{\alpha a^2}\right] \qquad (B1.1)$$

$$S_2 = S_2(y, y_o, \tau) = 1 + 2 \sum_{m=1}^{\infty} \cos\frac{m\pi y}{b} \cos\frac{m\pi y_o}{b} \, exp\left[-\frac{m^2\pi^2 k_y \tau}{\alpha b^2}\right] \qquad (B1.2)$$

$$S_3 = \sum_{l=1}^{\infty} \cos(2l+1)\frac{\pi z_0}{h} \cos(2l+1)\frac{\pi z}{h} \, exp\left[-\frac{(2l+1)^2\pi^2 k_z \tau}{4\alpha h^2}\right] \qquad (B2.1)$$

These Green's functions can be expressed as:

$$S_1 S_2 S_3 = \left[1 + 2 \sum_{n=1}^{\infty} \cos\frac{n\pi x}{a} \cos\frac{n\pi x_o}{a} \, exp\left(-\frac{n^2\pi^2 k_x \tau}{\alpha a^2}\right) \right.$$

$$+ 2 \sum_{m=1}^{\infty} \cos\frac{m\pi y}{b} \cos\frac{m\pi y_o}{b} \, exp\left(-\frac{m^2\pi^2 k_y \tau}{\alpha b^2}\right)$$

$$+ 4 \sum_{\substack{n=1 \\ m=1}}^{\infty} \cos\frac{n\pi x}{a} \cos\frac{n\pi x_o}{a} \cos\frac{m\pi y}{b} \cos\frac{m\pi y_o}{b} \, exp\left(-\frac{n^2\pi^2 k_x \tau}{\alpha a^2}\right.$$

$$\left. \left. -\frac{m^2\pi^2 k_y \tau}{\alpha b^2}\right) \right] \sum_{l=1}^{\infty} \cos(2l+1)\frac{\pi z_0}{h} \cos(2l$$

$$+ 1)\frac{\pi z}{h} \, exp\left[-\frac{(2l+1)^2\pi^2 k_z \tau}{4\alpha h^2}\right] \qquad (B2.2a)$$

$$S_1 S_2 S_3 = \sum_{l=1}^{\infty} \cos(2l+1)\frac{\pi z_0}{h}\cos(2l+1)\frac{\pi z}{h}\,exp\left[-\frac{(2l+1)^2\pi^2 k_z\tau}{4\alpha h^2}\right]$$

$$+ 2\sum_{\substack{n=1 \\ l=1}}^{\infty} \cos\frac{n\pi x}{a}\cos\frac{n\pi x_o}{a}\cos(2l+1)\frac{\pi z}{h}\cos(2l+1)\frac{\pi z_o}{h}\,exp\left(-\frac{n^2\pi^2 k_x\tau}{\alpha a^2}\right.$$

$$\left. -\frac{(2l+1)^2\pi^2 k_z\tau}{4\alpha h^2}\right)$$

$$+ 2\sum_{\substack{m=1 \\ l=1}}^{\infty} \cos\frac{m\pi y}{b}\cos\frac{m\pi y_o}{b}\cos(2l+1)\frac{\pi z}{h}\cos(2l+1)\frac{\pi z_o}{h}\,exp\left(-\frac{m^2\pi^2 k_y\tau}{\alpha b^2}\right.$$

$$\left. -\frac{(2l+1)^2\pi^2 k_z\tau}{4\alpha h^2}\right)$$

$$+ \cos\frac{m\pi y_o}{b}\,exp\left(-\frac{m^2\pi^2 k_y\tau}{\alpha b^2}\right)$$

$$+ 4\sum_{\substack{n=1 \\ m=1 \\ l=1}}^{\infty} \cos\frac{n\pi x}{a}\cos\frac{n\pi x_o}{a}\cos\frac{m\pi y}{b}\cos\frac{m\pi y_o}{b}\cos(2l+1)\frac{\pi z}{h}\cos(2l$$

$$+ 1)\frac{\pi z_o}{h}\,exp\left(-\frac{n^2\pi^2 k_x\tau}{\alpha a^2}-\frac{m^2\pi^2 k_y\tau}{\alpha b^2}-\frac{(2l+1)^2\pi^2 k_z\tau}{4\alpha h^2}\right) \qquad (B2.2b)$$

$$\int_{z_1}^{z_2} S_1 \, S_2 \, S_3 \, dz_o$$

$$= \frac{h}{\pi(2l+1)} \sum_{l}^{\infty} \cos(2l+1)\frac{\pi z}{h}\left[\sin\frac{(2l+1)\pi z_2}{h}\right.$$

$$\left. - \sin\frac{(2l+1)\pi z_1}{h}\right] exp\left(-\frac{(2l+1)^2\pi^2 k_z\tau}{4\alpha h^2}\right)$$

$$+ \frac{2h}{\pi(2l+1)} \sum_{\substack{n=1 \\ l=1}}^{\infty} \cos\frac{n\pi x}{a}\cos\frac{n\pi x_o}{a}\cos(2l$$

$$+ 1)\frac{\pi z}{h}\left[\sin\frac{(2l+1)\pi z_2}{h} - \sin\frac{(2l+1)\pi z_1}{h}\right] exp\left(-\frac{n^2\pi^2 k_x\tau}{\alpha a^2} - \frac{(2l+1)^2\pi^2 k_z\tau}{4\alpha h^2}\right)$$

$$+ \frac{2h}{\pi(2l+1)} \sum_{\substack{m=1 \\ l=1}}^{\infty} \cos\frac{m\pi y}{b}\cos\frac{m\pi y_o}{b}\cos(2l$$

$$+ 1)\frac{\pi z}{h}\left[\sin\frac{(2l+1)\pi z_2}{h} - \sin\frac{(2l+1)\pi z_1}{h}\right] exp\left(-\frac{m^2\pi^2 k_y\tau}{\alpha b^2} - \frac{(2l+1)^2\pi^2 k_z\tau}{4\alpha h^2}\right)$$

$$+ \frac{4h}{\pi(2l+1)} \sum_{\substack{n=1 \\ m=1 \\ l=1}}^{\infty} \cos\frac{n\pi x}{a}\cos\frac{n\pi x_o}{a}\cos\frac{m\pi y}{b}\cos\frac{m\pi y_o}{b}\cos(2l$$

$$+ 1)\frac{\pi z}{h}\left[\sin\frac{(2l+1)\pi z_2}{h} - \sin\frac{(2l+1)\pi z_1}{h}\right] exp\left(-\frac{n^2\pi^2 k_x\tau}{\alpha a^2} - \frac{m^2\pi^2 k_y\tau}{\alpha b^2}\right.$$

$$\left. - \frac{(2l+1)^2\pi^2 k_z\tau}{4\alpha h^2}\right) \qquad\qquad (B2.3a)$$

$$\int_0^t \int_{z_1}^{z_2} (S_1.S_2.S_3)\, d_{zo} d_\tau$$

$$= \frac{4\alpha h^3}{\pi^3 (2l+1)^3 k_z} \sum_l^\infty cos(2l+1) \frac{\pi z}{h} \left[\sin\frac{(2l+1)\pi z_2}{h} - \sin\frac{(2l+1)\pi z_1}{h}\right] \Bigg(1$$

$$- exp\left(-\frac{\pi^2 t}{4\alpha}\left(\frac{(2l+1)^2 k_z}{h^2}\right)\right)\Bigg)\Bigg)$$

$$+ \frac{8\alpha h}{\pi^3 (2l+1)\left(\frac{4n^2 k_x}{a^2} + \frac{(2l+1)^2 k_z}{h^2}\right)} \sum_{\substack{n=1 \\ l=1}}^\infty cos\frac{n\pi x}{a} cos\frac{n\pi x_o}{a} cos(2l$$

$$+ 1)\frac{\pi z}{h}\left[\sin\frac{(2l+1)\pi z_2}{h} - \sin\frac{(2l+1)\pi z_1}{h}\right]\left(1 - exp\left(-\frac{\pi^2 t}{4\alpha}\left(\frac{4n^2 k_x}{a^2} + \frac{(2l+1)^2 k_z}{h^2}\right)\right)\right)\Bigg)$$

$$+ \frac{8\alpha h}{\pi^3 (2l+1)\left(\frac{4m^2 k_y}{b^2} + \frac{(2l+1)^2 k_z}{h^2}\right)} \sum_{\substack{m=1 \\ l=1}}^\infty cos\frac{m\pi y}{b} cos\frac{m\pi y_o}{b} cos(2l$$

$$+ 1)\frac{\pi z}{h}\left[\sin\frac{(2l+1)\pi z_2}{h} - \sin\frac{(2l+1)\pi z_1}{h}\right]\left(1 - exp\left(-\frac{\pi^2 t}{4\alpha}\left(\frac{4m^2 k_y}{b^2} + \frac{(2l+1)^2 k_z}{h^2}\right)\right)\right)\Bigg)$$

$$+ \frac{16\alpha h}{\pi^3 (2l+1)\left(\frac{4n^2 k_x}{a^2} + \frac{4m^2 k_y}{b^2} + \frac{(2l+1)^2 k_z}{h^2}\right)} \sum_{n=m=l}^\infty cos\frac{n\pi x}{a} cos\frac{n\pi x_o}{a} cos\frac{m\pi y}{b} cos\frac{m\pi y_o}{b} cos(2l$$

$$+ 1)\frac{\pi z}{h}\left[\sin\frac{(2l+1)\pi z_2}{h} - \sin\frac{(2l+1)\pi z_1}{h}\right]\Bigg(1$$

$$- exp\left(-\frac{\pi^2 t}{4\alpha}\left(\frac{4n^2 k_x}{a^2} + \frac{4m^2 k_y}{b^2} + \frac{(2l+1)^2 k_z}{h^2}\right)\right)\Bigg)\Bigg) \qquad\qquad (B2.3b)$$

$$\Delta P = (P_i - P)$$

$$= \left[\frac{886.9 B\mu q}{abhL\alpha}\right]\left[\frac{4\alpha h^3}{\pi^3(2l+1)^3 k_z}\sum_{l}^{\infty}\cos(2l+1)\frac{\pi z}{h}\left[\sin\frac{(2l+1)\pi z_2}{h} - \sin\frac{(2l+1)\pi z_1}{h}\right]\left(1\right.\right.$$

$$\left.\left. - exp\left(-\frac{\pi^2 t}{4\alpha}\left(\frac{(2l+1)^2 k_z}{h^2}\right)\right)\right)\right)$$

$$+ \frac{8\alpha h}{\pi^3(2l+1)\left(\frac{4n^2 k_x}{a^2} + \frac{(2l+1)^2 k_z}{h^2}\right)}\sum_{\substack{n=1 \\ l=1}}^{\infty}\cos\frac{n\pi x}{a}\cos\frac{n\pi x_o}{a}\cos(2l$$

$$+ 1)\frac{\pi z}{h}\left[\sin\frac{(2l+1)\pi z_2}{h} - \sin\frac{(2l+1)\pi z_1}{h}\right]\left(1 - exp\left(-\frac{\pi^2 t}{4\alpha}\left(\frac{4n^2 k_x}{a^2} + \frac{(2l+1)^2 k_z}{h^2}\right)\right)\right)$$

$$+ \frac{8\alpha h}{\pi^3(2l+1)\left(\frac{4m^2 k_y}{b^2} + \frac{(2l+1)^2 k_z}{h^2}\right)}\sum_{\substack{m=1 \\ l=1}}^{\infty}\cos\frac{m\pi y}{b}\cos\frac{m\pi y_o}{b}\cos(2l$$

$$+ 1)\frac{\pi z}{h}\left[\sin\frac{(2l+1)\pi z_2}{h} - \sin\frac{(2l+1)\pi z_1}{h}\right]\left(1 - exp\left(-\frac{\pi^2 t}{4\alpha}\left(\frac{4m^2 k_y}{b^2} + \frac{(2l+1)^2 k_z}{h^2}\right)\right)\right)$$

$$+ \frac{16\alpha h}{\pi^3(2l+1)\left(\frac{4n^2 k_x}{a^2} + \frac{4m^2 k_y}{b^2} + \frac{(2l+1)^2 k_z}{h^2}\right)}\sum_{n=m=l}^{\infty}\cos\frac{n\pi x}{a}\cos\frac{n\pi x_o}{a}\cos\frac{m\pi y}{b}\cos\frac{m\pi y_o}{b}\cos(2l$$

$$+ 1)\frac{\pi z}{h}\left[\sin\frac{(2l+1)\pi z_2}{h} - \sin\frac{(2l+1)\pi z_1}{h}\right]\left(1\right.$$

$$\left.\left. - exp\left(-\frac{\pi^2 t}{4\alpha}\left(\frac{4n^2 k_x}{a^2} + \frac{4m^2 k_y}{b^2} + \frac{(2l+1)^2 k_z}{h^2}\right)\right)\right)\right] \qquad (B2.4)$$

This is the pressure drop at any point (x,y,z) inside the reservoir at time t.

For pseudo steady state (large time) behaviour of delta P in the above, let time t go to infinity and drop all factors in the exponential terms.

$$P_i - P(x, y, z; t \to \infty)$$

$$= \left[\frac{886.9 B\mu q}{abhL\alpha}\right]\left[\frac{4\alpha h^3}{\pi^3(2l+1)^3 k_z}\sum_{l}^{\infty}\cos(2l+1)\frac{\pi z}{h}\left[\sin\frac{(2l+1)\pi z_2}{h} - \sin\frac{(2l+1)\pi z_1}{h}\right]\right.$$

$$+ \frac{8\alpha h}{\pi^3(2l+1)\left(\frac{4n^2 k_x}{a^2} + \frac{(2l+1)^2 k_z}{h^2}\right)}\sum_{\substack{n=1 \\ l=1}}^{\infty}\cos\frac{n\pi x}{a}\cos\frac{n\pi x_o}{a}\cos(2l$$

$$+ 1)\frac{\pi z}{h}\left[\sin\frac{(2l+1)\pi z_2}{h} - \sin\frac{(2l+1)\pi z_1}{h}\right]$$

$$+ \frac{8\alpha h}{\pi^3(2l+1)\left(\frac{4m^2 k_y}{b^2} + \frac{(2l+1)^2 k_z}{h^2}\right)}\sum_{\substack{m=1 \\ l=1}}^{\infty}\cos\frac{m\pi y}{b}\cos\frac{m\pi y_o}{b}\cos(2l$$

$$+ 1)\frac{\pi z}{h}\left[\sin\frac{(2l+1)\pi z_2}{h} - \sin\frac{(2l+1)\pi z_1}{h}\right]$$

$$+ \frac{16\alpha h}{\pi^3(2l+1)\left(\frac{4n^2 k_x}{a^2} + \frac{4m^2 k_y}{b^2} + \frac{(2l+1)^2 k_z}{h^2}\right)}\sum_{n=m=l}^{\infty}\cos\frac{n\pi x}{a}\cos\frac{n\pi x_o}{a}\cos\frac{m\pi y}{b}\cos\frac{m\pi y_o}{b}\cos(2l$$

$$\left.+ 1)\frac{\pi z}{h}\left[\sin\frac{(2l+1)\pi z_2}{h} - \sin\frac{(2l+1)\pi z_1}{h}\right]\right] \qquad (B2.5)$$

By averaging equation (B2.5), over the entire reservoir region $0 \le x \le a, 0 \le y \le b, 0 \le z \le h$, we obtain average to zero identically

$$P_i - \bar{P}_R = 0 \qquad (B2.6)$$

Now, subtracting (B2.6) from (B2.5), we have:

$$\Delta P = (\bar{P}_R - P) = \left[\frac{886.9 B\mu q}{abhL}\right]\left[P_z + P_{xz} + P_{yz} + P_{xyz}\right] \qquad (B2.7)$$

Where:

$$P_z = \frac{4h^3}{\pi^3 k_z}\sum_{l=1}^{\infty}\frac{\cos(2l+1)\frac{\pi z}{h}\left[\sin\frac{(2l+1)\pi z_2}{h} - \sin\frac{(2l+1)\pi z_1}{h}\right]}{(2l+1)^3} \qquad (B2.8)$$

$$P_{xz} = \frac{8h}{\pi^3}\sum_{n,l=1}^{\infty}\frac{\cos\frac{n\pi x}{a}\cos\frac{n\pi x_o}{a}\cos(2l+1)\frac{\pi z}{h}\left[\sin\frac{(2l+1)\pi z_2}{h} - \sin\frac{(2l+1)\pi z_1}{h}\right]}{(2l+1)\left(\frac{4n^2 k_x}{a^2} + \frac{(2l+1)^2 k_z}{h^2}\right)} \qquad (B2.9)$$

$$P_{yz} = \frac{8h}{\pi^3} \sum_{\substack{m=1 \\ l=1}}^{\infty} \frac{\cos\frac{m\pi y}{b} \cos\frac{m\pi y_o}{b} \cos(2l+1)\frac{\pi z}{h}\left[\sin\frac{(2l+1)\pi z_2}{h} - \sin\frac{(2l+1)\pi z_1}{h}\right]}{(2l+1)\left(\frac{4m^2 k_y}{b^2} + \frac{(2l+1)^2 k_z}{h^2}\right)} \quad \text{(B2.10)}$$

P_{xyz}

$$= \frac{16h}{\pi^3} \sum_{n,m,l}^{\infty} \frac{\cos\frac{n\pi x}{a} \cos\frac{n\pi x_o}{a} \cos\frac{m\pi y}{b} \cos\frac{m\pi y_o}{b} \cos(2l+1)\frac{\pi z}{h}\left[\sin\frac{(2l+1)\pi z_2}{h} - \sin\frac{(2l+1)\pi z_1}{h}\right]}{(2l+1)\left[\frac{4n^2 k_x}{a^2} + \frac{4m^2 k_y}{b^2} + \frac{(2l+1)^2 k_z}{h^2}\right]}$$

$$\text{(B2.11)}$$

The flowing point source functions from Gringarten and Ramey are used.

Recall S_3 from Appendix B2;

$$S_1 = \sum_{n=1}^{\infty} \cos(2n+1)\frac{\pi x_0}{a}\cos(2n+1)\frac{\pi x}{a}\,exp\left[-\frac{(2n+1)^2\pi^2 k_x \tau}{4\alpha a^2}\right] \tag{B3.1}$$

$$S_2 = \sum_{m=1}^{\infty} \cos(2m+1)\frac{\pi y_0}{b}\cos(2m+1)\frac{\pi y}{b}\,exp\left[-\frac{(2m+1)^2\pi^2 y\tau}{4\alpha b^2}\right] \tag{B3.2}$$

$$S_3 = \sum_{l=1}^{\infty} \cos(2l+1)\frac{\pi z_0}{h}\cos(2l+1)\frac{\pi z}{h}\,exp\left[-\frac{(2l+1)^2\pi^2 k_z \tau}{4\alpha h^2}\right] \tag{B2.1}$$

$$S_1.S_2.S_3 = \sum_{n;m;l=1}^{\infty} \cos(2n+1)\frac{\pi x_0}{a}\cos(2n+1)\frac{\pi x}{a}\cos(2n+1)\frac{\pi y}{b}\cos(2n+1)\frac{\pi x y_0}{b}\cos(2l$$

$$+1)\frac{\pi z_0}{h}\cos(2l+1)\frac{\pi z}{h}Exp\left[-\frac{\pi^2 t}{4\alpha}\left(\frac{(2n+1)^2 k_x}{a^2}+\frac{(2m+1)^2 k_y}{b^2}\right.\right.$$

$$\left.\left.+\frac{(2l+1)^2 k_z}{h^2}\right)\right] \tag{B3.3a}$$

$$\int_{z_1}^{z_2} S_1\, S_2\, S_3\, dz_o$$

$$= \frac{h}{\pi(2l+1)}\sum_{n,m,l}\cos(2n+1)\frac{\pi x_0}{a}\cos(2n$$

$$+1)\frac{\pi x}{a}\cos(2n+1)\frac{\pi y}{b}\cos(2n+1)\frac{\pi x y_0}{b}\cos(2l$$

$$+1)\frac{\pi z}{h}\left[\sin\frac{(2l+1)\pi z_2}{h}-\sin\frac{(2l+1)\pi z_1}{h}\right]exp\left[-\frac{\pi^2 t}{4\alpha}\left(\frac{(2n+1)^2 k_x}{a^2}\right.\right.$$

$$\left.\left.+\frac{(2m+1)^2 k_y}{b^2}+\frac{(2l+1)^2 k_z}{h^2}\right)\right] \tag{B3.3b}$$

$$\int_0^t \int_{z_1}^{z_2} (S_1 . S_2 . S_3) \, dz_o d_\tau$$

$$= \frac{4\alpha h}{\pi^3 (2l+1) \left[\frac{(2n+1)^2 k_x}{a^2} + \frac{(2m+1)^2 k_y}{b^2} + \frac{(2l+1)^2 k_z}{h^2} \right]} \sum_{n;m;l=1} \cos(2n$$

$$+ 1) \frac{\pi x_0}{a} \cos(2n+1) \frac{\pi x}{a} \cos(2n+1) \frac{\pi y}{b} \cos(2n+1) \frac{\pi x y_0}{b} \cos(2l$$

$$+ 1) \frac{\pi z}{h} \left[\sin \frac{(2l+1)\pi z_2}{h} - \sin \frac{(2l+1)\pi z_1}{h} \right] \Big| 1$$

$$- \exp\left(-\frac{\pi^2 t}{4\alpha} \left(\frac{(2n+1)^2 k_x}{a^2} + \frac{(2m+1)^2 k_y}{b^2} \right. \right.$$

$$\left. \left. + \frac{(2l+1)^2 k_z}{h^2} \right) \right) \Big]$$

$$(B3.3c)$$

$$\Delta P = (P_i - P)$$

$$= \left[\frac{886.9 B\mu q}{abhL\alpha} \right] \frac{4\alpha h}{\pi^3 (2l+1) \left[\frac{(2n+1)^2 k_x}{a^2} + \frac{(2m+1)^2 k_y}{b^2} + \frac{(2l+1)^2 k_z}{h^2} \right]} \sum_{n;l=1} \cos(2n$$

$$+ 1) \frac{\pi x}{a} \cos(2n+1) \frac{\pi x_0}{a} \cos(2n+1) \frac{\pi y}{b} \cos(2n+1) \frac{\pi x y_0}{b} \cos(2l$$

$$+ 1) \frac{\pi z}{h} \left[\sin \frac{(2l+1)\pi z_2}{h} - \sin \frac{(2l+1)\pi z_1}{h} \right] \Big[1$$

$$- \exp\left(-\frac{\pi^2 t}{4\alpha} \left(\frac{(2n+1)^2 k_x}{a^2} + \frac{(2m+1)^2 k_y}{b^2} + \frac{(2l+1)^2 k_z}{h^2} \right) \right) \Big]$$

$$(B3.4)$$

Equation (B3.4) is the pressure drop at any point (x,y,z) inside the reservoir at time t,

For pseudo steady state (large time) behaviour of ΔP in the above equation, we let $t \to \infty$ and drop all terms with exponential factors;

$$P_i - P(x,y,z;t \to \infty)$$

$$= \left[\frac{886.9 B\mu q}{abh(Z_2 - Z_1)\alpha} \right] \frac{4\alpha h}{\pi^3 (2l+1) \left[\frac{(2n+1)^2 k_x}{a^2} + \frac{(2m+1)^2 k_y}{b^2} + \frac{(2l+1)^2 k_z}{h^2} \right]} \sum_{n;l=1} \cos(2n$$

$$+ 1) \frac{\pi x_0}{a} \cos(2n+1) \frac{\pi x}{a} \cos(2n+1) \frac{\pi y}{b} \cos(2n+1) \frac{\pi x y_0}{b} \cos(2l$$

$$+ 1) \frac{\pi z}{h} \left[\sin \frac{(2l+1)\pi z_2}{h} - \sin \frac{(2l+1)\pi z_1}{h} \right]$$

$$(B3.5)$$

By averaging the equation above over the entire reservoir region $0 \leq x \leq a, 0 \leq y \leq b, \ 0 \leq z \leq h$, we obtain all the terms in the summation average to zero identically;

Therefore the equation becomes:

$$P_i - \bar{P}_R = 0 \qquad\qquad (B3.6)$$

Now subtracting equation (B3.6) from equation (B3.5), yields the general formula for the pseudo steady state pressure drop at an arbitrary point (x,y,z) in the reservoir;

$$(\bar{P}_R - P) =$$

$$\left[\frac{886.9 B \mu q}{abh(z_2 - z_1)}\right] \frac{4h}{\pi^3} \sum_{n,m,l}^{\infty} \frac{\cos(2n+1)\frac{\pi x}{a}\cos(2n+1)\frac{\pi x_0}{a}\cos(2n+1)\frac{\pi y}{b}\cos(2n+1)\frac{\pi x y_0}{b}\cos(2l+1)\frac{\pi z}{h}\left[\sin\frac{(2l+1)\pi z_2}{h}-\sin\frac{(2l+1)\pi z_1}{h}\right]}{(2l+1)\left[\frac{(2n+1)^2 k_x}{a^2}+\frac{(2m+1)^2 k_y}{b^2}+\frac{(2l+1)^2 k_z}{h^2}\right]}$$

$$(B3.7)$$